Journal of Hydrology 590 (2020) 125336

Contents lists available at ScienceDirect

Journal of Hydrology

journal homepage: www.elsevier.com/locate/jhydrol

Research papers

Agricultural water optimization coupling with a distributed ecohydrological model in a mountain-plain basin

Farong Huang[a,b,d], Xingguo Mo[b,c,*], Shi Hu[b], Lanhai Li[a,d]

[a] State Key Laboratory of Desert and Oasis Ecology, Xinjiang Institute of Ecology and Geography, Chinese Academy of Sciences, Urumqi 830011, China
[b] Key Laboratory of Water Cycle and Related Land Surface Processes, Institute of Geographic Sciences and Natural Resources Research, Chinese Academy of Sciences, Beijing 100101, China
[c] College of Resources and Environment/Sino-Danish Center, University of Chinese Academy of Sciences, Beijing 100049, China
[d] Ili Station for Watershed Ecosystem Research, Chinese Academy of Sciences, Xinyuan 835800, China

ARTICLE INFO

This manuscript was handled by Corrado Corradini, Editor-in-Chief, with the assistance of Weiping Chen, Associate Editor

Keywords:
Agricultural water optimization
VIP model
Natural runoff
Crop photosynthetic capacity
Crop water production function

ABSTRACT

Agricultural water optimization at the basin scale is critical for sustainable irrigated agriculture and water resources management. Crop Water Production Function (CWPF) and surface water are key components of agricultural water optimization. CWPF relates closely to crop yield/growth-related parameters, and surface water of sub-basins is often different and impacted by water withdrawals. However, CWPF accounting for the crop yield-related parameter and natural runoff of sub-basins were scarcely involved in agricultural water optimization at the basin scale. To fill this gap, CWPFs of different water units are estimated using a distributed ecohydrological model involving the spatial heterogeneity of crop photosynthetic capacity parameter, and the natural runoff of sub-basins is reproduced by this model. Integrating these functions and variables, and taking the agricultural benefit of the whole basin as the main objective, an agricultural water optimization model at the basin scale (AWOMB) is developed and applied to a mountain-plain basin in North China. The results showed that agricultural water optimization in a representative year would lead to 0.4% increase of crop production for the whole basin at the expense of certain urban ecological water and equity of agricultural water. In this scenario, the river ecological water requirements in all sub-basins would be satisfied. Assuming the domestic, industrial and river ecological water demand being fully satisfied in 2020s, water deficits will be 8% and 26% for the whole basin under the normal and dry year scenarios, respectively. Correspondingly, increments of 2% and 7% crop production are predicted in these two scenarios by agricultural water optimization. It is demonstrated that water resources utilization and agricultural production are effectively improved by coupling a distributed ecohydrological model with water resources optimization in the study basin. This research provides a methodology for integrative catchment water resources management.

1. Introduction

Agriculture consumes about 70% of the water resources in the world (Schlager, 2005; Galán-Martín et al., 2017). Under the influence of agricultural irrigation, the streamflow in Central Asia, Southwest Europe, Middle East Pakistan, Northwest China and North China has decreased (Cai et al., 2002; Yang and Tian, 2009; Siddiqi and Wescoat, 2013; Liu et al., 2015; Jiang et al., 2016; Vicente-Serrano et al., 2019). The runoff decrease in upper catchments in these arid, semi-arid or semi-humid regions led to groundwater overexploitation and even river drying up in the lower catchments, and consequently runoff into the terminal lakes or seas decreased (Wang et al., 2008; Guo and Shen, 2015; Mekonnen et al., 2015; Xu et al., 2019). On the other hand, irrigation dominates grain production in these regions (Deng et al., 2006; Jiang et al., 2015; Hasson et al., 2019), where agricultural irrigation poses a great challenge on the sustainability of water utilization and agricultural production. Since agricultural water optimization may effectively support both food and water sustainability by increasing water productivity (Brauman et al., 2013; Jiang et al., 2016; Smilovic et al., 2019), it is required for sustainable water management and agricultural production in arid, semi-arid or semi-humid regions with water stress at the basin scale.

Optimization models are essential tools of agricultural water optimization. These models are generally based on traditional

* Corresponding author at: Key Laboratory of Water Cycle and Related Land Surface Processes, Institute of Geographic Sciences and Natural Resources Research, Chinese Academy of Sciences, Beijing 100101, China.
E-mail address: moxg@igsnrr.ac.cn (X. Mo).

https://doi.org/10.1016/j.jhydrol.2020.125336
Received 10 April 2020; Received in revised form 1 July 2020; Accepted 21 July 2020
Available online 04 August 2020

Nomenclature

$Agre_t$ agricultural benefit for the whole basin in year t
$CWPF_{kt}$ crop water production function for unit k in year t (kg)
Eco_t ecological benefit for the whole basin in year t
EQ_t equity of agricultural water for the whole basin in year t
ET_a annual actual ET (mm)
GDP_{indok} industrial GDP in unit k in a given year (10^4Yuan)
GDP_{indkt} industrial GDP in unit k in year t (10^4Yuan)
I_{ak} area of irrigated farm in unit k (ha)
I_{Rkt} annual actual irrigation in unit k in year t (mm)
irr_{kt} satisfaction ratio of agricultural water in unit k in year t
irr_{mt} average irr_{kt} for all units in year t
$irrWUE_{kt}$ irrigation water use efficiency in unit k in year t (kg ha^{-1} mm^{-1})
I_{skt} average sufficient irrigation for all grids of irrigated farm in unit k in year t (mm)
k unit number
k_basin sub-basin including unit k which is not a separate sub-basin
k_sub separate sub-basin included in k_basin
k_0, k_1 first and last number for k_sub
K_{citykt}, $K_{ruralkt}$ urban and rural domestic water quota in unit k in year t (L day^{-1}person^{-1})
k_s, k_e the first and last number of upper units for unit k
n number of years for prediction
n_{dayt} total days in year t
nu number of water units
Obj_t integrated objective function of the water optimization in year t
P_{citykt}, $P_{ruralkt}$ urban and rural population in unit k in year t
P_{eff} effective monthly precipitation (mm month^{-1})
P_{kt} total population in unit k in year t
P_{month} monthly precipitation (mm month^{-1})
P_{ok} population in unit k in a given year
P_{valid} effective annual precipitation (mm)
Q_{indkt} water consumption per 10^4 Yuan GDP in unit k in year t (m^3 (10^4Yuan)$^{-1}$)
q_n urban ecological water quota (m^3 year^{-1} person^{-1})
R_{gkt} annual groundwater supply not double counting in the surface water of unit k in year t (m^3)
R_{nkt} natural runoff generated in unit k in year t (m^3)
R_{nkt_basin} reproduced natural runoff of k_basin in year t (m^3)
R_{nkt_sub} reproduced natural runoff of k_sub in year t (m^3)
$r_{otherkt}$ ratio of $W_{otherkt}$ to the sum of W_{lifekt}, W_{indkt}, W_{ekt} and W_{agrakt}
S_{amin}, S_{cmin} minimum satisfaction ratio of agricultural and urban ecological water demand
S_{kt} annual surface water supply of unit k in year t (m^3)
t year number
U_{kt} urbanization rate in unit k in year t
vi averaged growth rate of industrial GDP (10^4Yuan year^{-1})
v_k natural population growth rate in unit k
w_1, w_2, w_3 weight of $Agre_t$, Eco_t, EQ_t
W_{agrakt} gross annual actual agricultural water in unit k in year t (m^3)
W_{agrkt} annual agricultural water demand of unit k in year t (m^3)
W_{agrskt} gross annual sufficient irrigation water of unit k in year t (m^3)
W_{citykt}, $W_{ruralkt}$ annual urban and rural domestic water demand in unit k in year t (m^3)
W_{ckt} annual urban ecological water demand of unit k in year t (m^3)
W_{ekt} annual ecological water demand of unit k in year t (m^3)
W_{indkt} annual industrial water demand of unit k in year t (m^3)
W_{kt} annual water supply of unit k in year t (m^3)
W_{lifekt} annual domestic water demand of unit k in year t (m^3)
W_{okt} annual other water supply of unit k in year t (m^3)
$W_{otherkt}$ water used by other sectors of unit k in year t (m^3)
W_{outkt} outflow of unit k in year t (m^3)
W_{rkt} annual river ecological water demand of unit k in year t (m^3)
W_{ukt} annual residue water of the upper units for unit k in year t (m^3)
X_{kt} gross agricultural water allocated to unit k in year t (m^3)
$Yield\max_{kt}$ average yield with sufficient irrigation for all grids of irrigated farm in unit k in year t (kg ha^{-1})
$Yield_{\min kt}$ average rainfed yield for all grids of irrigated farm in unit k in year t (kg ha^{-1})
Y_{kt} urban ecological water allocated to unit k in year t (m^3)
α_{kt} effective irrigation water utilization rate in unit k in year t
η_{indkt} reuse rate of industrial water in unit k in year t

programming method, such as linear programming (LP), nonlinear programming and fractional programming (Ahrends et al., 2008; Garcia-Vila and Fereres, 2012; Garg and Dadhich, 2014; Jiang et al., 2016; Zhao et al., 2017; Sadeghi et al., 2020); uncertain programming method, such as stochastic optimization, robust programming, fractile optimization, fuzzy programming, interval programming and chance-constrained programming (Wang and Huang, 2015; Yang et al., 2015; Zeng et al., 2017; Dai et al., 2018; Dong et al., 2018; Tan and Zhang, 2018; Li et al., 2019a, 2019b); heuristic optimization algorithm, such as genetic algorithm (GA) and ant colony optimization (Cai et al., 2002; Alvarez et al., 2004; Nguyen et al., 2017; Wen et al., 2017; Li et al., 2020b); and other optimization methods, such as particle swarm optimization, game model and pattern search algorithm (Su et al., 2014; Fu et al., 2019; Linker, 2020). A few scholars have carried out agricultural water resources optimization at the basin scale with the optimization models mentioned above. For example, Sadeghi et al. (2020) designated the optimal agricultural management pattern from the view of water-energy-food nexus at the basin scale with a LP model; Ahrends et al. (2008) optimized the irrigation cultivation in a semi-arid catchment of West Africa using the nonlinear programming; and Su et al. (2014) conducted the agricultural water resources optimal allocation with the pattern search algorithm based on subdivision of virtual water into blue and green virtual water in Shiyang River Basin in Northwest China. Further, GA is one of the frequently used techniques to obtain the optimal water scheme (Li et al., 2020b), and this method can be applied to many complex problems that are difficult to solve using traditional gradient-based approaches (Goldberg, 1989; Michalewicz, 1994; Montesinos et al., 2001).

Optimization models are commonly constrained with available water resources, agricultural water demand or irrigated area, aiming to maximize the benefit for the study area (Ahrends et al., 2008; Garcia-Vila and Fereres, 2012; Su et al., 2014; Yang et al., 2015; Jiang et al., 2016; Dang et al., 2018). The available water resources used in the optimization models are normally for the whole study area, either derived from the statistical information or hydrological modeling (Ahrends et al., 2008; Garcia-Vila and Fereres, 2012; Su et al., 2014; Dang et al., 2018). Although the streamflow shows spatial difference in a watershed and the observed streamflow is reduced due to withdrawing for irrigation (Yang and Tian, 2009; Zuo and Chen, 2012; Li et al., 2020a), the natural runoff of sub-basins is scarcely included in the agricultural water optimization. In addition, the response of crop yield to water in the optimization models is ordinarily based on empirical relationships (Garg and Dadhich, 2014; Yang et al., 2015). However, the empirical relationship describing the response of crop

yield to irrigation (i.e. the crop water production function (CWPF)) is inappropriate in a different environment (Saseendran et al., 2015).

The process-based crop or agro-hydrological model can describe the dynamic process of agro-ecosystem well and is convenient to consider environmental parameters. This kind of model has been used to investigate the spatial patterns of crop productivity and water use efficiency under climate change and to raise management strategies (such as cropping structure) based on scenario analysis of several pre-specified alternatives (Singh et al., 2006; Mo et al., 2009; Jiang et al., 2015; Xue and Ren, 2017; Yu et al., 2017). A few researchers have used these kinds of models to derive CWPFs under different climate and soil conditions (Garcia-Vila and Fereres, 2012; Saseendran et al., 2015; Jiang et al., 2016; Smilovic et al., 2019). Some of them even utilized the derived CWPFs in water resources optimization models (Garcia-Vila and Fereres, 2012; Jiang et al., 2016). Considering crop yield is a key variable in CWPF and crop yield is sensitive to growth/production-related parameters in agro-ecosystem model (Zhang et al., 2020), CWPF derived from modelling will be impacted by the growth/production-related parameters. Crop photosynthetic capacity belongs to this kind of parameters (Mo et al., 2005b), and it shows spatial heterogeneity due to the impact of soil nitrogen (Brück and Guo, 2006; Hu and Mo, 2011; Li et al., 2019a, 2019b). However, CWPF accounting for the spatial difference of crop growth/production-related parameters (such as crop photosynthetic capacity) has not been used in the agricultural water optimization at the basin scale.

The Vegetation Interface Processes (VIP) model is a process-based distributed ecohydrological model based on grids. The VIP model can effectively describe the impact of the spatial heterogeneity of photosynthetic capacity on crop yield and the relationship between yield and irrigation (Hu et al., 2010, 2014, 2019; Hu and Mo, 2011). The VIP model can also successfully simulate the river streamflow in different basins (Mo et al., 2005a; Huang and Mo, 2015; Wang et al., 2015), as well as the natural runoff in the basin with intensified irrigation (Huang and Mo, 2015). Since the runoff generation and runoff routing in VIP model is based on grids, it can reproduce the streamflow of different sub-basins simultaneously. In this work, we will use the VIP model to derive the natural runoff of sub-basins, as well as the CWPF accounting for the spatial heterogeneity of crop photosynthetic capacity.

The objective of this study is to improve crop yield and outflow in a basin, thus an agricultural water optimization model at the basin scale (AWOMB) solving by GA is developed. The AWOMB takes agricultural benefit as the main objective function, and this function is constructed with the CWPF retrieved with the VIP ecohydrological dynamic model. Furthermore, the natural runoff of sub-basins from VIP model is taken as critical parameter of constraints in the AWOMB. Using the Hutuo River Basin (HRB) in North China as an example, agricultural water optimization is conducted at the basin scale under different water supply and demand scenarios, and the response of crop yield and outflow is explored.

2. Study area and data

2.1. Study area

Ziya River Basin (112°13′-116°03′, 36°17′-39°28′) is located in the southern part of Haihe River Basin in North China, including Fuyang River and Hutuo River (Fig. 1a). Hutuo River Basin (HRB) is taken as the study area due to its dendritic drainage. Taking the outlet at Huangbizhuang, the upper reach of HRB is mainly located in Xinzhou and Yangquan in Shanxi Province, covering an area of 2.3×10^4 km^2.

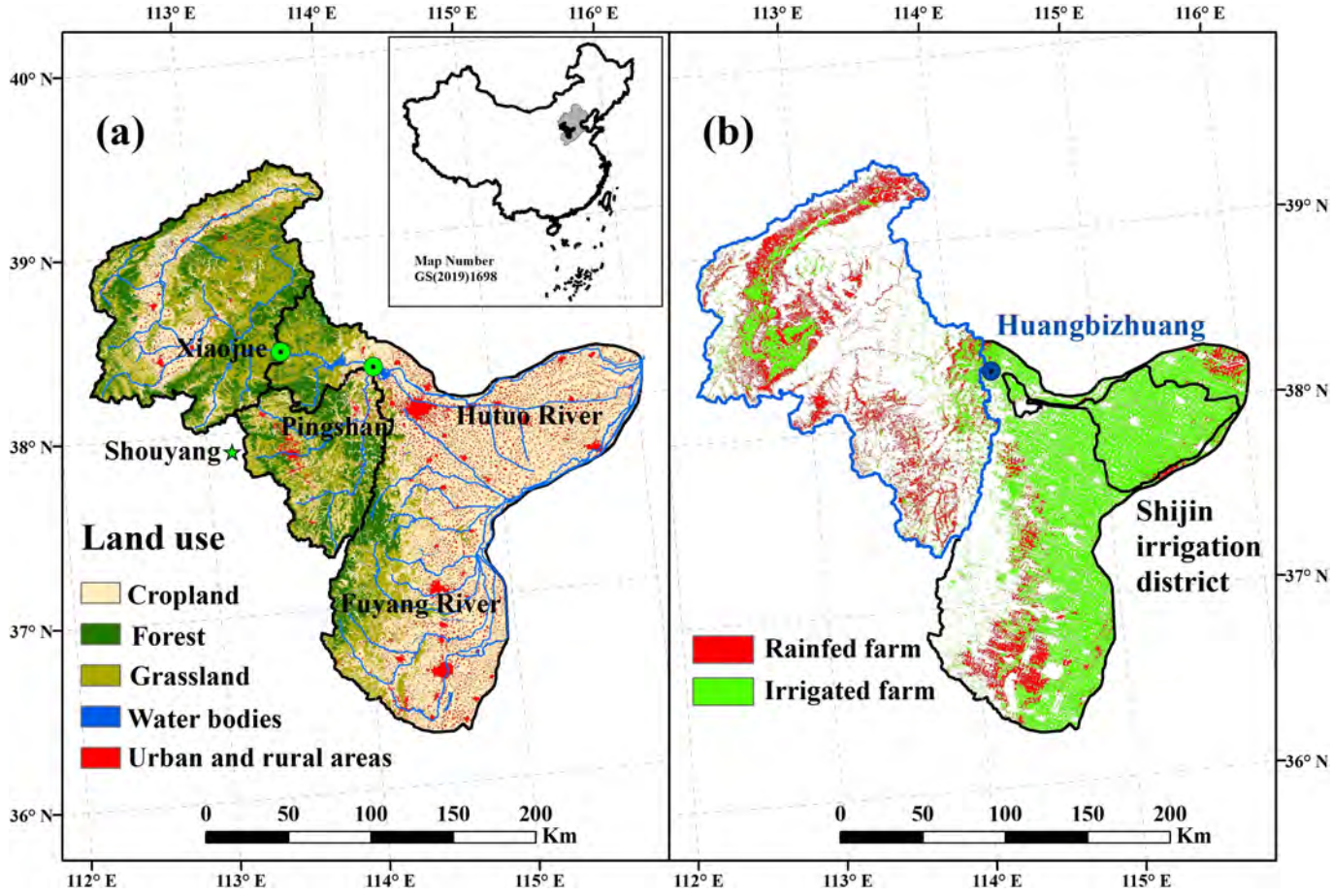

Fig. 1. (a) Land use, location of hydrological stations and (b) irrigated farm in the Ziya River Basin.

The lower reach (Shijin District) primarily lies in Shijiazhuang and Hengshui in Hebei Province, with an area of 4, 346 km^2 (Fig. 1b). The climate in HRB belongs to continental monsoon climate, with annual average temperature of 10.8℃ and accumulated precipitation of 513 mm. The precipitation shows large spatial and temporal variability. For example, annual precipitation in Wutai Mountain in the upper reach is about 631 mm, while it is about 505 mm in the lower reach. Approximately 80% of annual precipitation occurs in July, August and September, and the maximum range of annual precipitation is above 300 mm during 1956–2013. Land use types mainly include cropland, forest, grassland and water bodies, with cropland taking up 35% (Fig. 1a). The main crop in the upper reach is spring maize, while the lower reach is dominated by the annual double-crop rotation system of winter wheat and summer maize (Kendy et al., 2003; Sun et al., 2010).

2.2. Data

The data in this work include the geographic information data, remote sensing data, meteorological data, hydrological data, agricultural data, and socioeconomic data. The geographic information, remote sensing vegetation index and meteorological data are mainly used to drive the VIP model, and the measurements of river discharge are used for model calibration during 1956–1959 and validation during 1960–1979. The agricultural and socioeconomic data (Table 1) are mainly employed in the water demand calculation.

The geographic information composes of topography, land use, and soil texture data. The digital evaluation model (DEM) data with a spatial resolution of 30 m from US Geological Survey database is used to describe the topography. Land use data from TM images around 2010, at the scale of 1:100,000 (http://www.resdc.cn/), is utilized. Soil texture is classified with the sand, silt and clay percent fractions (1:1,000,000) from the second soil survey of China (http://westdc.westgis.ac.cn/data/8a8f3ac3-d628-4d20-a815-487c2ac9c373). The DEM is processed to the required spatial resolution (250 m) in Lambert projection with the bilinear resample method, while land use and soil texture data with the majority resample method.

Remote sensing data used in this work includes the Terra-Modis 16-days maximum composite Normalized Difference Vegetation Index (NDVI) from 2001 to 2013, at 250 m resolution. All the NDVI images have been conducted for projection transformation (Lambert projection), geometrical and atmospheric correction, and Savtzky-Golay (S-G) filter (Savitzky and Golay, 1964).

The meteorological data during 1956–2013 is from the China Meteorological Data Service Center (http://data.cma.cn/en), including daily variables of air temperatures (mean, maximum and minimum), water vapor pressure, wind speed, sunshine duration, and precipitation recorded at 78 national meteorological stations in and around the study area. The meteorological data is spatially interpolated to 250 m resolution with the gradient inverse distance (GIDS) method (Lin et al., 2002). The hydrological data from Annual Hydrological Report of China consists of monthly streamflow during 1956–1979 of two stations in HRB (Xiaojue and Pingshan, Fig. 1a).

The agricultural data includes the effective irrigation ratio of farmland, effective irrigation water utilization rate, and crop yield in 2005–2013 for each county in the study area. The socioeconomic data primarily includes groundwater and other water resources data, urbanization rate, population, natural population growth rate, and GDP in 1999–2013.

3. Methodology

Using the data above, an AWOMB model is constructed coupling with a distributed ecohydrological model (i.e. the VIP model) (Fig. 2) in the mountain-plain basin, so as to alleviate the water scarcity and guarantee the agricultural productivity.

3.1. The VIP model

The VIP model is a physical-process-based ecosystem dynamic model and can simulate the exchanges of energy, water, and carbon between the terrestrial ecosystem and the atmosphere at each grid of the land surface (Mo et al., 2017). Based on the secondary derivations of the differences between leaf/ground temperature and air temperature, the energy budgets of vegetation canopy and soil surface are estimated separately with the Penman-Monteith equation. In the canopy, short wave radiation transferring is separated into visible and near infrared components (Mo et al., 2018). Regarding water budgets, land surface runoff generation is described with a modified variable infiltration capacity equation, accounting for the daily net precipitation and moisture deficit to saturation in the upper-soil layer. Simulation of soil water movement is implemented with the discrete Richards equation. The groundwater recharge from the soil is calculated with the Darcy Law. The drainage of groundwater to channels is simulated with two (namely the upper and lower) linear reservoirs. The overland and channel runoff routing is computed based on the kinematic wave equation solved by a one-dimensional four point finite backward-difference method. According to the water and energy balance, land surface evapotranspiration (ET) is derived. ET consists of three components, namely vegetation transpiration, evaporation from soil surface, and canopy interception (Mo et al., 2005a). In the carbon cycle scheme, photosynthetic production is calculated based on the biochemical schemes for C3 (Farquhar et al., 1980) and C4 plants (Collatz et al., 1992) respectively, then up-scaled to canopy with vertical profiles of sunlit and shaded leaves groups. The photosynthetic production is the

Table 1
Data in the representative year (2007).

Data	Source	Value	Unit
Surface water of Hebei province	www.china.com.cn	152	10^8 m^3
Ground water of Shijiazhuang	Water resources development of Hebei Province in the early 21st century	18	10^8 m^3
Ground water of Yangquan/Xinzhou	Water resources bulletin of Shanxi	0.61/3.11	10^8 m^3
Other water resources of Shijiazhuang	Li et al. (2007)	2.4	10^8 m^3
Other water resources of Yangquan/Xinzhou	Water resources bulletin of Shanxi	0.45/0.08	10^8 m^3
Natural population growth rate of Shanxi/Hebei	Statistical yearbook	0.5%/0.7%	
Averaged growth rate of industrial GDP	Statistical yearbook	8.5%	
Water consumption per 10^4 Yuan GDP in Shanxi/ Hebei	Water resources bulletin of Shanxi/Fu (2012)	81/115	m^3 $(10^4 Yuan)^{-1}$
Reuse rate of industrial water	Water resources bulletin of Shanxi	0.3	
Urban/rural domestic water quota	Water resources bulletin of Shanxi	52/41	L $day^{-1}person^{-1}$
Urbanization rate	Fu (2012)	0.34	
Ratio of other water demand in Shanxi/Shijiazhuang	Water resources bulletin of Shanxi/Shijiazhuang	0.08/0.12	
Effective irrigation water utilization rate in Xinzhou/other parts of the study area	Zhang (2009)	0.4/0.43	

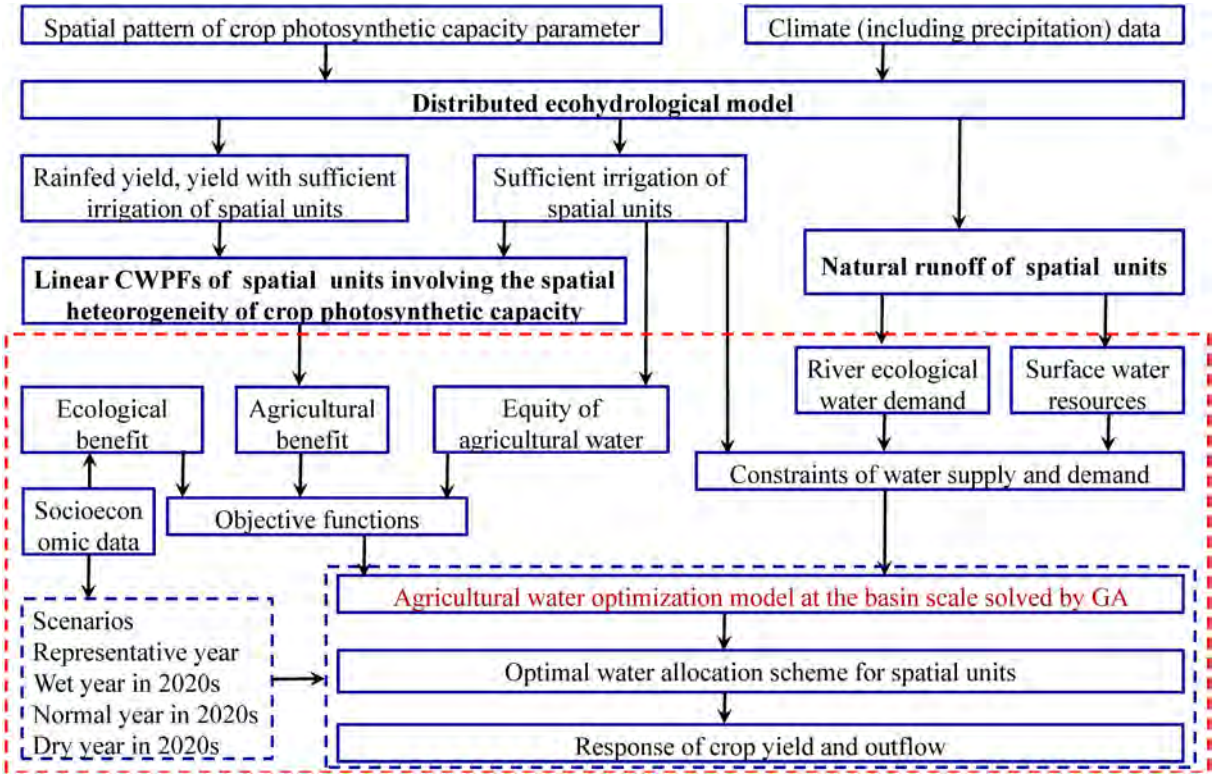

Fig. 2. Study framework. GA-Genetic Algorithm. CWPF-crop water production function.

input variables of the crop growth module for biomass and leaf area estimation. In the crop growth module, crop phenological stages are expressed with air temperature degree–day which determines the fractions of assimilation partitioned to crop components (leaf, stem, root and grain), and crop yield is sensitive to the photosynthetic capacity parameter. The spatial patterns of two photosynthetic capacity parameters (i.e. maximum Rubisco catalytic capacity of winter wheat and intrinsic quantum efficiency of spring maize) have been retrieved with remote sensing information (Hu et al., 2014, 2019). In terms of the interaction among water cycle, energy transfer and carbon cycle, transpiration, stomatal conductance and photosynthesis are coupled via leaf stomatal conductance-photosynthesis relationship in the VIP model (Ball et al., 1987; Mo et al., 2009).

3.2. Water supply and demand of each unit in the AWOMB

In this study, the water units in the upstream (Fig. 3) are derived based on the sub-basins obtained with DEM and the outlet stations with reported drainage area in Annual Hydrological Report of China. The small sub-basin is taken as a separate water unit, while the area not included in any small sub-basin but included in a large sub-basin is also taken as a water unit. The water unit in the downstream is Shijin District, with discharge from the mountain outlet reservoirs as one of the water sources.

For unit k in year t, its annual water supply W_{kt} (m^3) includes surface water S_{kt} (m^3), groundwater not double counting in the surface water R_{gkt} (m^3) and other water W_{okt} (such as collecting rainwater,

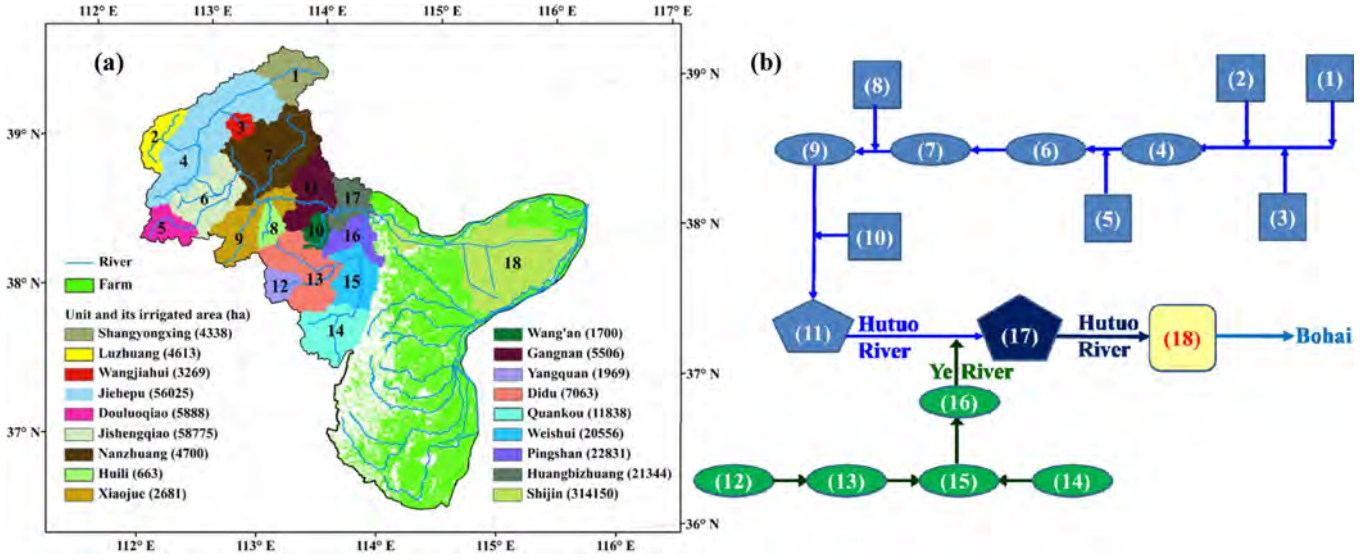

Fig. 3. Agricultural water units in the Hutuo River basin (unit 1–9 locate in Xinzhou, unit 12–14 locate in Yangquan, others locate in Hebei Province).

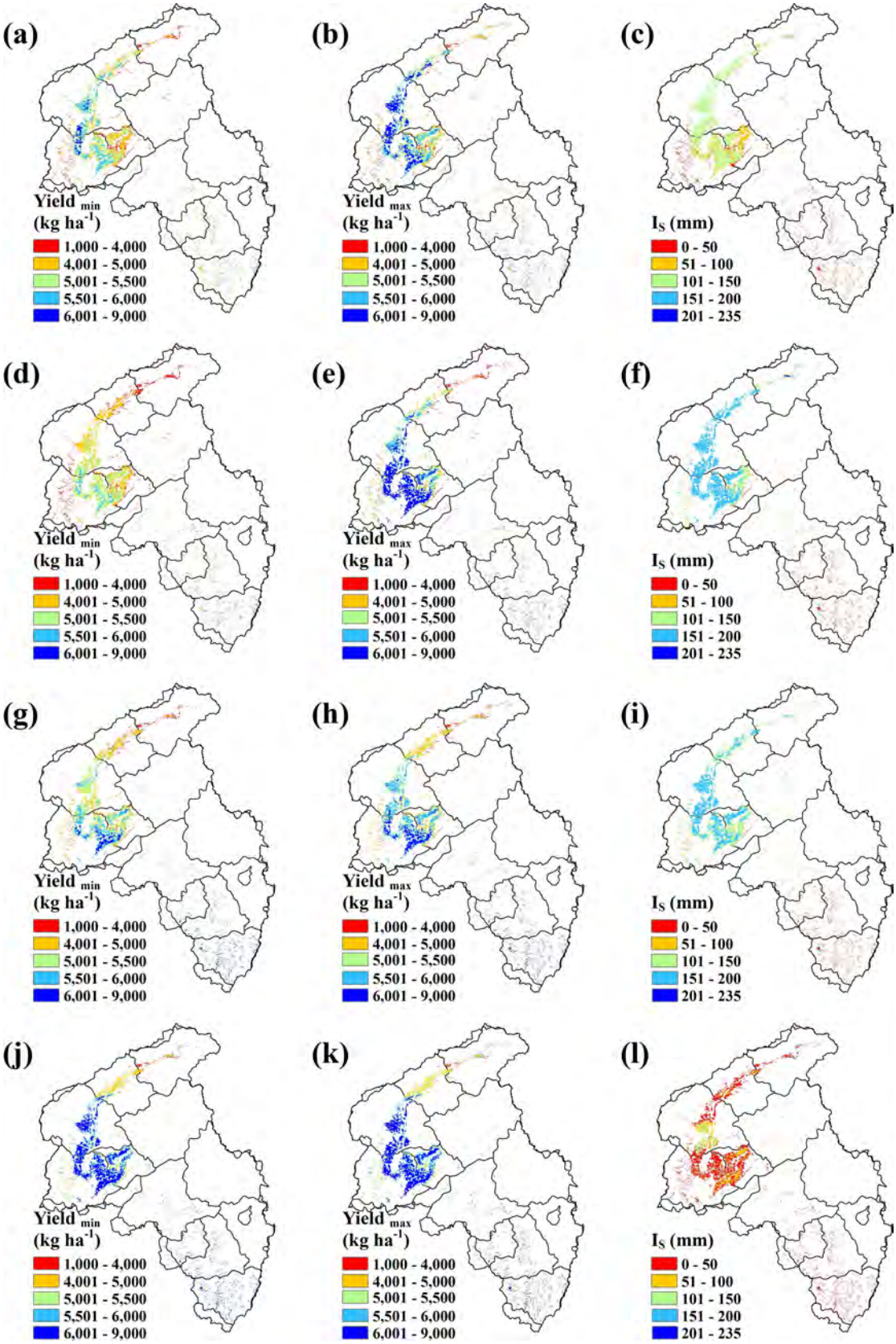

Fig. 4. Rainfed yield ($Yield_{min}$), yield with sufficient irrigation ($Yield_{max}$) and sufficient irrigation (I_s) estimated by VIP model for spring maize on irrigated farm in the representative year (a, b, c), dry year (d, e, f), normal year (g, h, i) and wet year (j, k, l).

reclaimed water and water diverted from outside basins, m^3):

$$W_{kt} = S_{kt} + R_{gkt} + W_{okt} \quad (1)$$

Here, R_{gkt} and W_{okt} are calculated as the multiple of the reported water resources for the region including unit k and the area ratio of unit k to that region (namely the area ratio method). In this study, we assume the residual water in the upper units can reach the lower unit via the hydrographic net for irrigation purpose. Therefore, S_{kt} is the sum of the residual water of the upper units W_{ukt} (m^3) and the natural runoff generated in unit k R_{nkt} (m^3):

$$S_{kt} = R_{nkt} + W_{ukt} \quad (2)$$

Here R_{nkt} in the upstream units is predicted by the VIP model (Appendix A), while that in the downstream unit (Shijin District) is obtained with the area ratio method. W_{ukt} is calculated by the water balance method among units:

$$W_{ukt} = \sum_{k=k_s}^{k=k_e} (W_{kt} - W_{lifekt} - W_{indkt} - W_{ekt} - W_{agrkt} - W_{otherkt}) \quad (3)$$

where k_s and k_e indicate the first and last number of upper units for unit k. For unit k in year t, W_{lifekt} (m^3) represents the annual domestic water demand; W_{indkt} (m^3) denotes the industrial water demand; W_{ekt} (m^3) refers to the ecological water demand (including natural ecological water, namely river ecological water W_{rkt} (m^3) derived from the simulated natural runoff by the VIP model, and the ecological water outside river channels that primarily contains urban ecological water W_{ckt} (m^3) in this work); W_{agrkt} (m^3) is the agricultural (irrigation) water demand (the maximum value is derived by the VIP model, and the actual value is derived based on remotely sensed NDVI (Mo et al., 2015); and $W_{otherkt}$ (m^3) is the water used by other sectors (such as urban public water, water used by forest, livestock and fishery). See Appendix B for details on calculating W_{lifekt}, W_{indkt}, W_{ekt} and W_{agrkt}. $W_{otherkt}$ is acquired according to the following equation:

$$W_{otherkt} = \frac{W_{lifekt} + W_{indkt} + W_{ekt} + W_{agrakt}}{r_{otherkt}} \quad (4)$$

Here, W_{agrakt} (m^3) is the gross annual actual agricultural water for unit k in year t, and $r_{otherkt}$ is the ratio of $W_{otherkt}$ to the sum of W_{lifekt}, W_{indkt}, W_{ekt} and W_{agrakt}.

In order to guarantee the basic social and economic benefits of the basin, W_{lifekt}, W_{indkt} and $W_{otherkt}$ are assumed to be satisfied; in order to maintain the water network for the whole basin, W_{rkt} is also assumed to be satisfied. The agricultural water and urban ecological water of each unit will be optimized at the basin scale. For all water use sectors except agriculture, it is assumed that there is no water loss during water delivery.

3.3. Objective function of the AWOMB

Referring to Cai (1999), Su et al. (2014) and Dai et al. (2018), the objective functions of the AWOMB in year t include agricultural benefit ($Agre_t$), ecological benefit (Eco_t) and social benefit (i.e. equity of agricultural water, EQ_t) for the whole basin.

(1) $Agre_t$ is expressed as the relative production of the allocated agricultural water,

$$Agre_t = \max\left(\frac{\sum_{k=1}^{k=nu} CWPF_{kt}(X_{kt}, \alpha_{kt})}{\sum_{k=1}^{k=nu} Yield_{\max kt} \times I_{ak}}\right) \quad (5)$$

where nu is the total number of units (nu is 18 in this work), $CWPF_{kt}$ (kg) is the CWPF for unit k in year t, X_{kt} (m^3) is the gross agricultural water allocated to unit k, α_{kt} is the effective irrigation water utilization rate in unit k, $Yield_{maxkt}$ (kg ha^{-1}) is the average yield with sufficient irrigation for all grids of irrigated farm in unit k, and I_{ak} (ha) is the area of irrigated farm in unit k (Appendix B). Assuming X_{kt} is evenly distributed in each grid of the irrigated farmland, $CWPF_{kt}$ is given by,

$$CWPF_{kt}(X_{kt}, \alpha_{kt}) = Yield_{\min kt} \times I_{ak} + \frac{irrWUE_{kt} \times (X_{kt} \times \alpha_{kt})}{10} \quad (6)$$

where $Yield_{minkt}$ (kg ha^{-1}) is the average rainfed yield for all grids of irrigated farmland in unit k, $irrWUE_{kt}$ (kg ha^{-1} mm^{-1}) is the irrigation water use efficiency in unit k, which can be expressed as follows (Bos, 1980, 1985):

$$irrWUE_{kt} = \frac{Yield_{\max kt} - Yield_{\min kt}}{I_{skt}} \quad (7)$$

where I_{skt} (mm) is the average sufficient irrigation for all grids of irrigated farm in unit k. $Yield_{maxkt}$, $Yield_{minkt}$ and I_{skt} are obtained with VIP model as follows.

The photosynthetic capacity parameter with spatial heterogeneity is

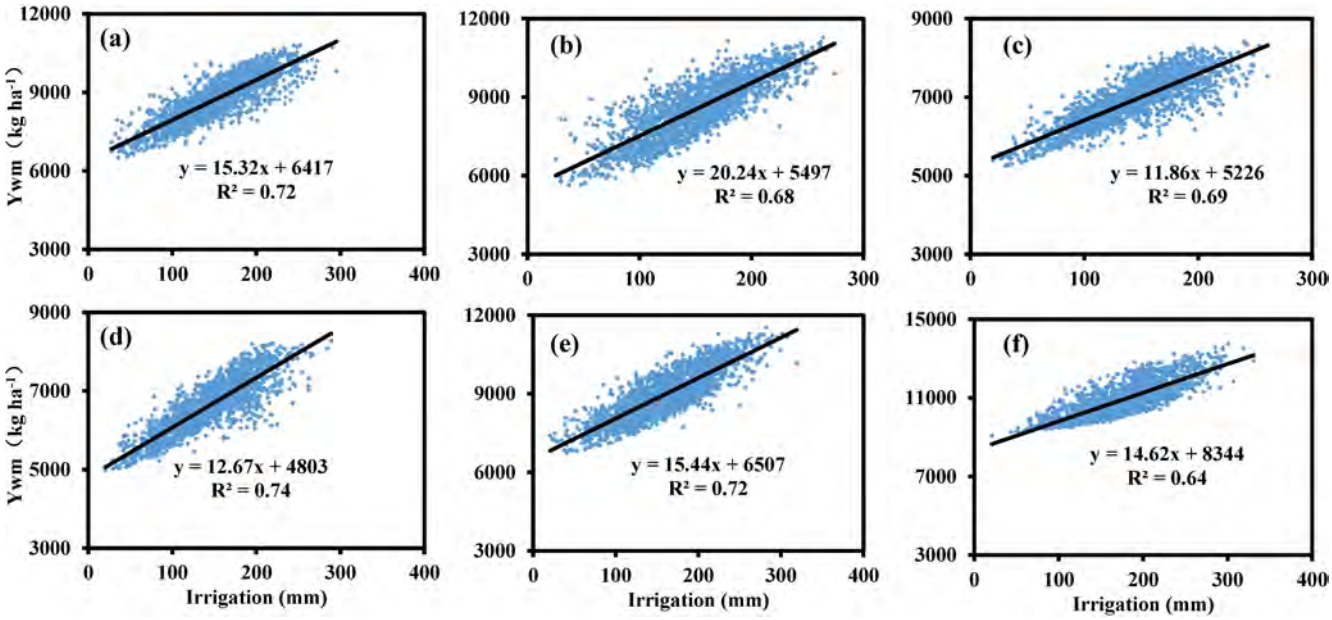

Fig. 5. Total irrigation and yield (Ywm) of winter wheat and summer maize estimated with VIP model based on the random experiemts in the representative year. (a), (b), (c), (d), (e) and (f) is for the representative grid in unit 10, 11, 15, 16, 17 and 18, respectively.

used to obtain the variables used in CWPF (i.e. $Yield_{maxkt}$, $Yield_{minkt}$ and I_{skt}). For spring maize in unit 1–9 and 12–14 in the mountainous area (Fig. 3), the spatial pattern of the critical photosynthetic capacity parameter (i. e. the intrinsic quantum efficiency, μmol C μmol^{-1} photons) is acquired from Hu et al. (2019). The spatial pattern of the intrinsic quantum efficiency is then used to simulate regional $Yield_{maxkt}$, $Yield_{minkt}$ and I_{skt} (Fig. 4) with the VIP model. Specifically, at each irrigated farm grid, $Yield_{minkt}$ is the rainfed yield; I_{skt} is the total irrigation water in the growing season, i.e. when the soil water in the root zone is below the field capacity, irrigation water is supplied to reach the field capacity; and the corresponding yield of I_{skt} is $Yield_{maxkt}$.

The winter wheat-summer maize units are mostly located in the plain area. The total $Yield_{maxkt}$, $Yield_{minkt}$ and I_{skt} for these two crops are acquired with the VIP model based on the random experiment method for the representative grid in unit k (10–11, 15–18), i.e. when the soil water in the root zone is below a random value in 45%-70% of the field capacity, irrigation water is supplied to reach another random value in 75%–100% of the field capacity. The photosynthetic capacity parameter of winter wheat (i.e. maximum catalytic capacity of Rubisco) for the representative grid is taken as the average value for irrigated farm grids in unit k (Hu et al., 2014). The other photosynthetic capacity parameters of winter wheat and summer maize are obtained according to Mo et al. (2009). Employing these photosynthetic capacity parameters, the random experiments are conducted for 2000 times with VIP model. The maximum irrigation of these experiments is I_{skt}. The intercept regressing linearly the yield with irrigation from random experiments is $Yield_{minkt}$, and the linear trend is the irrigation water use efficiency $irrWUE_{kt}$, as shown in Fig. 5. Using $irrWUE_{kt}$, I_{skt} and $Yield_{minkt}$, $Yield_{maxkt}$ is obtained based on Eq. (7).

(2) Due to the river ecological water of each unit being fully satisfied, Eco_t is expressed as the averaged satisfaction ratio of urban ecological water for all units:

$$Eco_t = \max\left(\frac{\sum_{k=1}^{k=nu}\frac{Y_{kt}}{W_{ckt}}}{nu}\right) \tag{8}$$

where Y_{kt} (m^3) is the urban ecological water allocated to unit k in year t.

(3) EQ_t is adopted as the standard error of the satisfaction ratio of agricultural water (Cai, 1999),

$$EQ_t = \min\left(\sqrt{\frac{\sum_{k=1}^{k=nu}(irr_{kt} - irr_{mt})^2}{n}}\right) \tag{9}$$

$$irr_{kt} = \frac{X_{kt}}{W_{agrskt}} \tag{10}$$

$$irr_{mt} = \frac{\sum_{k=1}^{k=nu} irr_{kt}}{n} \tag{11}$$

Here irr_{kt} is the satisfaction ratio of agricultural water of unit k in year t, irr_{mt} is the average irr_{kt} for all units, and W_{agrskt} (m^3) is the gross sufficient irrigation volume (Appendix B).

(4) This work aims to obtain maximum agricultural and ecological benefit as well as minimum difference in the agricultural water satisfaction ratio. Considering each objective function above is dimensionless ranging from 0 to 1, the integrated objective function of the water optimization in year t (Obj_t) is expressed as,

$$Obj_t = \max(w_1 \times Agre_t + w_2 \times Eco_t - w_3 \times EQ_t) \tag{12}$$

$$w_1 + w_2 + w_3 = 1 \tag{13}$$

where w_1, w_2 and w_3 represents the weight of $Agre_t$, Eco_t and EQ_t, being 0.8, 0.1 and 0.1 (Table 2), respectively. The weight is set according to the advice of experts based on the purpose of the agricultural water optimization model, namely to maximize agricultural benefit while considering social and ecological benefits. Further, the social and ecological benefits are considered equally important.

The optimization techniques have been used widely in agricultural water allocation (Singh, 2012). Among these techniques, GA focuses on the set of individuals, and its calculation is for all decision variables. GA is suitable for solving a multi-objective problem for the whole system, and it will be used to solve the multi-objective optimization problem constrained with equations below (Section 3.4) in the present study.

3.4. Constraints of the AWOMB

In this study, considering the available water supply in each unit, potential water demand of agriculture, potential water demand of urban ecological landscape, and inflow to the large reservoirs, constraints of the AWOMB are as follows:

(1) Total available water

In year t, for unit k (k = 1, 2, 3, …, 18), X_{kt} and Y_{kt} should be less than W_{kt} subtracted by the satisfied W_{lifekt}, W_{indkt}, W_{rkt} and $W_{otherkt}$,

$$X_{kt} + Y_{kt} \leqslant W_{kt} - W_{lifekt} - W_{indkt} - W_{rkt} - W_{otherkt} \tag{14}$$

(2) Allowable maximum and minimum allocated water of agricultural and urban ecological sectors

In year t, for unit k, both X_{kt} and Y_{kt} should fall in certain ranges,

$$S_{a\min} \times W_{agrskt} \leqslant X_{kt} \leqslant W_{agrskt} \tag{15}$$

$$S_{c\min} \times W_{ckt} \leqslant Y_{kt} \leqslant W_{ckt} \tag{16}$$

where S_{amin} and S_{cmin} is the minimum satisfaction ratio of agricultural water and urban ecological water, respectively. Considering that the water is insufficient in HRB, and assuming some river ecological water can be used as urban ecological water simultaneously, S_{amin} and S_{cmin} is set as 0.1 and 0.3 (Table 2).

(3) The inflow of the reservoir

For unit 11 and 17 with large reservoirs, the inflow from upper units should be larger than the river ecological water:

$$W_{ukt} \geqslant W_{rkt} \tag{17}$$

3.5. Implementation

Considering different water supply and demand situations as well as water resources regulation in HRB, four scenarios are set in this study, namely: the representative year with scarce water (2007), and wet, normal, dry year in 2020s with water delivery from South-to-North Water Transfer Project for the lower reach. Based on the precipitation time series in 1956–2013, we choose the year with annual precipitation of 75%, 50% and 25% guaranteed rate as the wet, normal and dry year in 2020s, respectively. The natural streamflow, agricultural water demand and crop yield in the corresponding year is then used in the agricultural water optimization. In 2020s, the other water resources (not including water delivery from South-to-North Water Transfer Project) will be calculated as 30% of the sum of urban domestic water and industrial water, and the effective irrigation water utilization rate will increase to 0.55 (Table 3). According to the reports of Shijin District Administration and Water Conservancy Bureau of Xinzhou, the irrigation structure has been greatly improved in recent years. Thus, the effective irrigation water utilization rate in 2020s is suitable. For the

Table 2
Parameters of the agricultural water optimization model.

Item	Value
Minimum satisfaction ratio of agricultural water	0.1
Minimum satisfaction ratio of urban ecological water	0.3
Weight of agricultural benefit	0.8
Weight of ecological benefit	0.1
Weight of social benefit	0.1

Table 3
Data used in 2020s.

Data	Source	Value	Unit
Water consumption per 10^4 Yuan GDP in Shanxi/Shijiazhuang	Calculated with fitted polynomial based on statistical data in 1999–2013	72/96	m^3 $(10^4Yuan)^{-1}$
Urbanization rate in Yangquan/Xinzhou /Shijiazhuang	Calculated with fitted polynomial based on statistical data in 1999–2013	0.63/0.41/0.49	
Urban/rural domestic water quota	Calculated with fitted polynomial based on statistical data in 1999–2013	51/46	L $day^{-1}person^{-1}$
Effective irrigation water utilization rate	Central Document No.1 in 2011	0.55	
South-to-North Water Diversion in Shijiazhuang	Li et al. (2007)	7.4	10^8 m^3

industrial water quota, urbanization rate and domestic water quota in 2020s, since the methods to derive them have been validated by the statistical data ($r > 0.70$, $p < 0.01$), the corresponding values in Table 3 are credible. In addition, according to our survey in Haihe River Water Conservancy Commission, the water delivery from South-to-North Water Transfer Project in 2020s will be carried out as plans. Therefore, the water delivery in Table 3 is rational. Except the data in Table 3, other data used in 2020s will be the same as that in the representative year.

In order to obtain the responses of yield and outflow to agricultural water optimization in 2020s, the situation without agricultural water optimization in 2020s is set as follows: the water resources of unit k is firstly used by the domestic, industrial, river ecological, and other water use sectors in this unit; then for the urban ecological water use sector in unit k; the third is the agricultural water use sector in unit k; and the last is the water use sectors in lower units of unit k. Based on the agricultural and urban ecological water before and after agricultural water optimization, the crop yield and outflow in response to agricultural water optimization are derived from Eqs. (6) and (18), respectively.

$$W_{outkt} = W_{kt} - W_{lifekt} - W_{indkt} - W_{otherkt} - X_{kt} - Y_{kt} + W_{rkt} \quad (18)$$

Here, W_{outkt} (m^3) is the outflow of unit k in year t.

4. Results

4.1. CWPF evaluation

CWPF is an important function used in the agricultural water optimization in this paper, which depicts the relationship between total crop yield and allocated irrigation water in a water unit. Prior to evaluating the regional CWPF of spring maize derived with VIP model, the modelling of spring maize has been validated with the observed data (Hu et al., 2019). The simulated above-ground biomass and leaf area index agree well with the observed value in 2011 ($r > 0.98$, $p < 0.01$) at the plot scale (Shouyang). The simulated yield of each county forced by the spatial pattern of the intrinsic quantum efficiency is consistent with the statistical yield ($r > 0.6$, $p < 0.01$) during 2005–2013 at the regional scale. Further, the sufficient irrigation in each spring maize unit under different scenarios is all less than 200 mm. Since the relationship between maize yield and irrigation is linear when the irrigation is less than 500 mm (Linker, 2020), the linear CWPF shown in Eq. (6) is valid for spring maize. According to the regional linear CWPF of spring maize accounting for the spatial heterogeneity of photosynthetic capacity, the average net actual irrigation of all counties is about 110 mm from 2005 to 2013, which is similar to the values reported in the water resources bulletin of Shanxi Province (114–134 mm). Therefore, the regional CWPF of spring maize derived from the VIP model is credible.

The derived CWPF of winter wheat-summer maize is evaluated via assessing variables used in CWPF in the representative year. The total sufficient irrigation used in CWPF is 330 mm (Table 4) in the Shijin District, which is consistent with the value (300–320 mm) reported by the Heibei Water Resources Department. In addition, the average sufficient irrigation of the winter wheat-summer maize units is 295 mm, which is close to the value (288 mm) reported by Ma et al. (2011) in the same area. The sufficient irrigation ranges from 261 to 330 mm in winter wheat-summer maize units (Table 4), which is similar to the optimal irrigation (240–330 mm) for sustainable water use (Hu et al., 2010). It indicates that the sufficient irrigation in this study represents the maximum irrigation in actual situation with limited water resources. Considering CWPF is linear when water supply for irrigation is limited (Zhao et al., 2017), the linear CWPF shown in Eq. (6) is rational for winter wheat-summer maize units. Furthermore, the total crop yield

Table 4
Yield and irrigation of each unit under different scenarios derived from VIP model.

	Representative year			Wet year in 2020s			Normal year in 2020s			Dry year in 2020s		
	Y_{min}	Y_{max}	I_s	Y_{min}	Y_{max}	I_s	Y_{min}	Y_{max}	I_s	Y_{min}	Y_{max}	I_s
Shangyongxing	3700	4142	124	4038	4107	17	3675	3937	136	2466	3354	165
Luzhuang	2920	3115	75	4752	4933	39	3992	4102	79	2411	2943	140
Wangjiahui	2904	3235	99	4957	5067	62	4441	4667	152	2046	2717	133
Jiehepu	5123	5583	126	5556	5654	53	4878	5184	167	4536	5527	177
Douluoqiao	3913	4099	37	5257	5315	24	4683	4808	104	3566	4279	127
Jishengqiao	4928	5340	109	5930	5973	35	5371	5585	155	4915	5854	164
Nanzhuang	3299	3629	54	5223	5361	45	4754	4961	140	2494	3057	92
Huili	4561	4994	79	6292	6340	28	5852	5943	120	4067	5085	92
Xiaojue	3347	3633	69	5770	5831	30	5227	5356	119	3162	3735	69
Yangquan	4708	4944	45	6215	6236	17	5682	5757	52	4789	5063	46
Didu	4359	4551	41	6194	6227	21	5632	5696	48	4540	4805	48
Quankou	5193	5402	52	6852	6939	17	6901	6969	43	5393	5686	42
Wang'an	6417	10,936	295	7669	9858	189	5803	8321	212	5346	11,516	271
Gangnan	5497	11,043	274	7548	10,027	195	5410	8555	239	5309	11,587	259
Weishui	5226	8321	261	6686	8477	161	5829	6794	175	5626	8776	218
Pingshan	4803	8465	289	6884	8162	141	6319	7532	153	4873	8553	248
Huangbizhuang	6507	11,448	320	8498	11,075	184	6248	9172	224	5346	11,470	272
Shijin	8344	13,169	330	11,897	14,476	155	9972	12,567	189	7431	13,378	281

Notes: Y_{min} – yield without irrigation (kg ha^{-1}), Y_{max} – yield with sufficient irrigation (kg ha^{-1}), I_s – sufficient irrigation (mm). The crop is winter whea-summer maize in Wang'an, Gangnan, Weishui, Pingshan, Huangbizhuang and Shijin unit, and it is spring maize in other units.

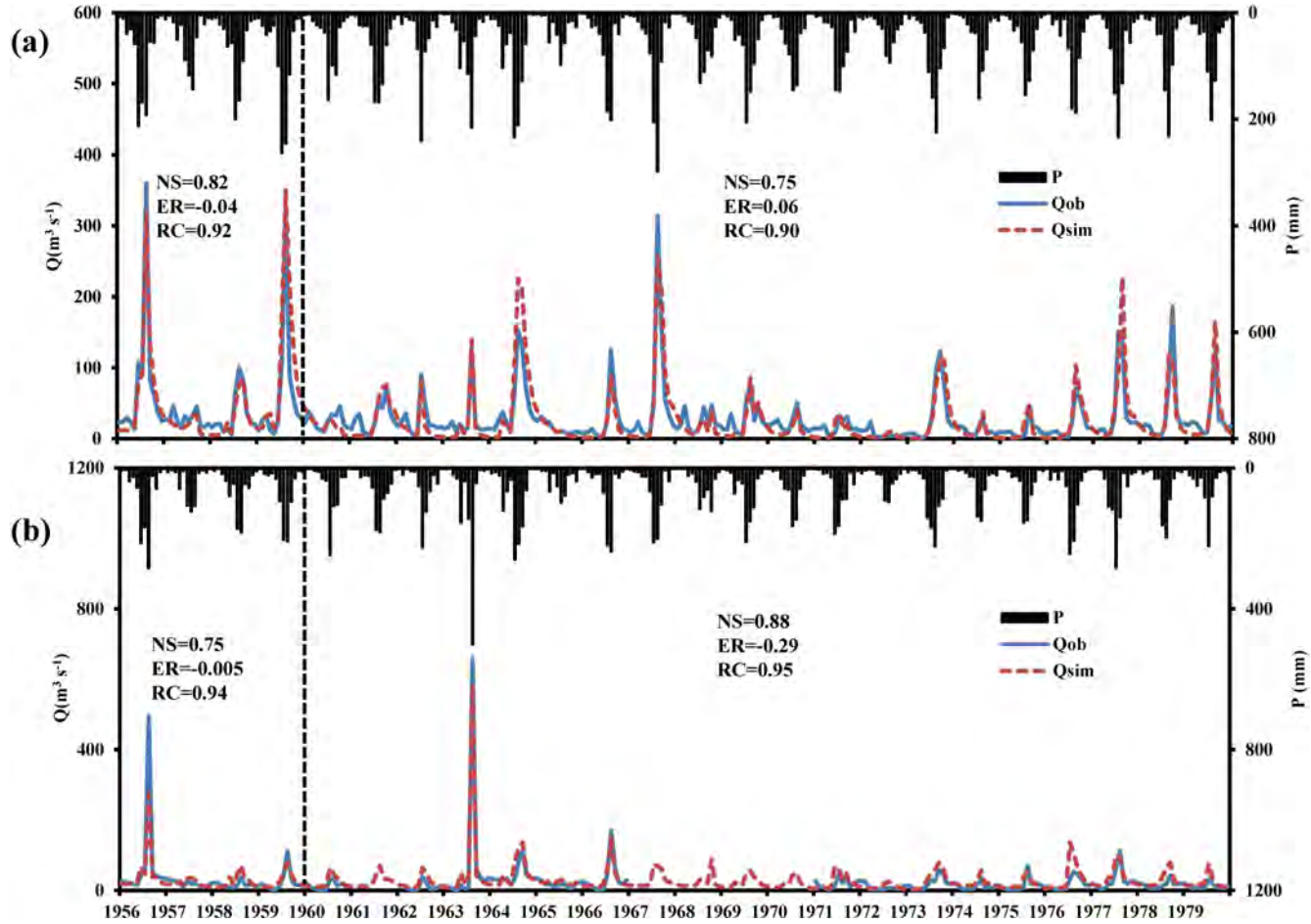

Fig. 6. Monthly streamflow of Xiaojue (a) and Pingshan (b). 'P' represents the monthly total precipitation.'Qob' and 'Qsim' represents the observed and simulated monthly average streamflow, respectively. 'NS' represents the Nash-Sutcliffe efficiency coefficient. 'ER' represents the relative volume error of the simulated stremflow to the observed value. 'RC' represents the correlation coefficient between the observed and simulated streamflow.

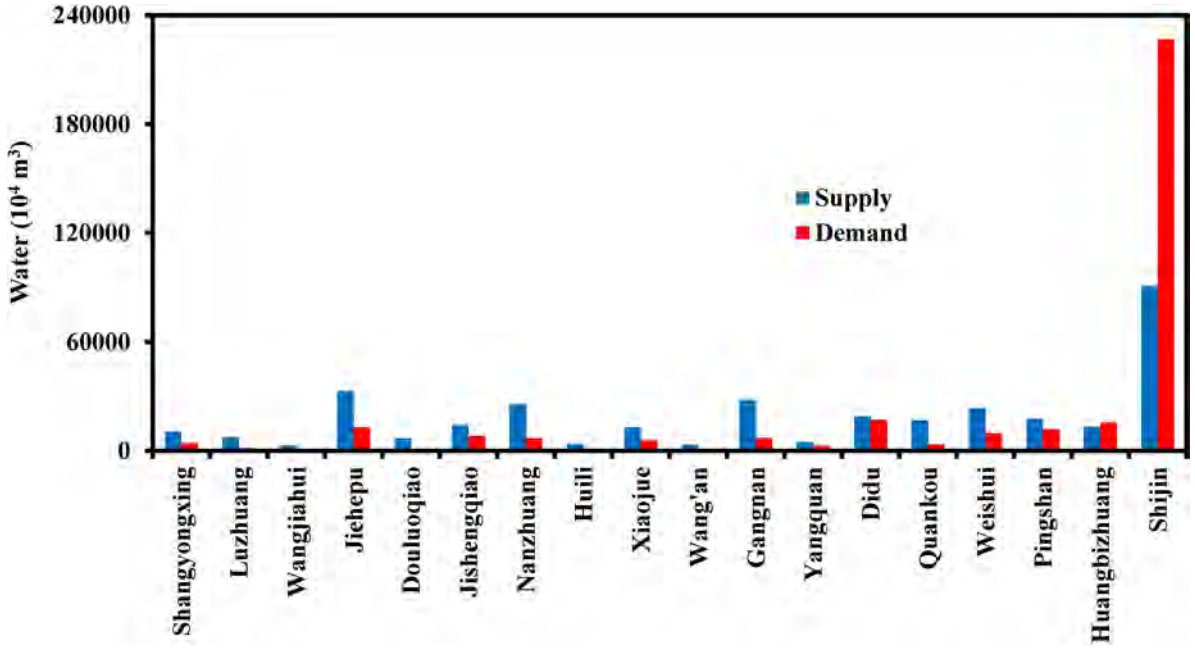

Fig. 7. Water supply and demand of each unit in the representative year.

Table 5
Agricultural water optimization in the representative year.

	R_n	W_{agra}	W_c	X	Y	Y_{act}	Y_{opt}	α_{sm}	V_{cmax}
Shangyongxing	9060	73	105	166	105	16,151	16,285	0.0339	
Luzhuang	6553	280	28	106	27	13,759	13,578	0.037	
Wangjiahui	2611	182	5	94	5	9736	9619	0.0425	
Jiehepu	28,215	2979	502	2065	159	291,341	290,032	0.0432	
Douluoqiao	5847	14	27	68	26	23,068	23,176	0.0354	
Jishengqiao	11,403	1678	457	1645	212	292,178	292,137	0.044	
Nanzhuang	21,977	174	200	74	67	15,926	15,686	0.047	
Huili	3255	29	23	21	23	3086	3067	0.0461	
Xiaojue	11,019	51	54	63	42	9059	9080	0.0409	
Yangquan	3658	49	206	33	74	9381	9344	0.0394	
Didu	14,339	263	561	87	189	31,315	30,960	0.039	
Quankou	12,993	1175	147	164	62	63,504	61,757	0.0438	
Wang'an	2794	213	7	118	6	12,308	11,716		100
Gangnan	8944	464	14	462	14	37,780	37,768		100
Weishui	8228	1667	176	1271	133	107,936	105,613		80
Pingshan	5055	3143	241	1537	241	122,348	113,574		80
Huangbizhuang	4522	3461	130	1953	69	160,748	151,298		100
Shijin	35,194	132,549	2656	141,297	884	3,510,842	3,554,737		120

Notes: R_n – natural runoff (10^4 m^3), W_{agra} – gross annual actual agricultural water (10^4 m^3), W_c – annual urban ecological water demand (10^4 m^3), X – gross agricultural water allocated to each unit (10^4 m^3), Y – urban ecological water allocated to each unit (10^4 m^3), Y_{act} –actual crop yield (ton) derived with W_{agra} and Equation (6) , Y_{opt} –crop yield after water optimization (ton), α_{sm}–average intrinsic quantum efficiency of spring maize (μmol C μmol^{-1} photons),V_{cmax}–average maximum catalytic capacity of Rubisco of winter wheat (μmol C m^{-2} s^{-1})

with sufficient irrigation employed in CWPF is 13169 kg ha^{-1} in the Shijin District. Referring to the regional yield simulated by VIP model (Lin, 2003; Hu et al., 2014), the corresponding value in Shijin District ranges from 12400 kg ha^{-1} to 13800 kg ha^{-1}. Hence, the predicted total crop yield with sufficient irrigation here is credible. However, the total yield with sufficient irrigation for winter wheat and summer maize in this study is less than the potential yield without water or nutrition stress (16300 kg ha^{-1}) (Mo et al., 2005b), because the photosynthetic capacity parameter here has accounted for the nutrition stress.

The variables employed in CWPF under different scenarios in 2020s (Table 4) are also analyzed. For winter wheat-summer maize unit, the total yield with sufficient irrigation is determined by the sum of precipitation and sufficient irrigation volume ($r > 0.79$, $p < 0.05$), particularly under the dry and normal year scenarios ($r > 0.87$, $p < 0.05$). For spring maize unit, the rainfed yield of irrigated farm is impacted not only by the precipitation but also the photosynthetic capacity parameter. The gap between the yield with sufficient irrigation and rainfed yield is dominated by the irrigation volume, particularly under the dry and normal year scenario ($r > 0.79$), indicating that maize yield is sensitive to drought, which is consistent with the results reported by other researchers (Potopova et al., 2015; Meng et al., 2016; Liu et al., 2017; Zdenek et al., 2017). Overall, the derived CWPFs are effective.

4.2. Natural runoff evaluation

The simulated natural runoff is firstly evaluated in the base period (1956–1979) with limited anthropogenic effects on river discharge (Yang and Tian, 2009; Huang and Mo, 2015). The results (Fig. 6) show that the simulated monthly value in the calibration period (1956–1960) and validation period (1961–1979) agreed well with the observed value for two different sub-basins. The Nash-Sutcliffe efficiency coefficients

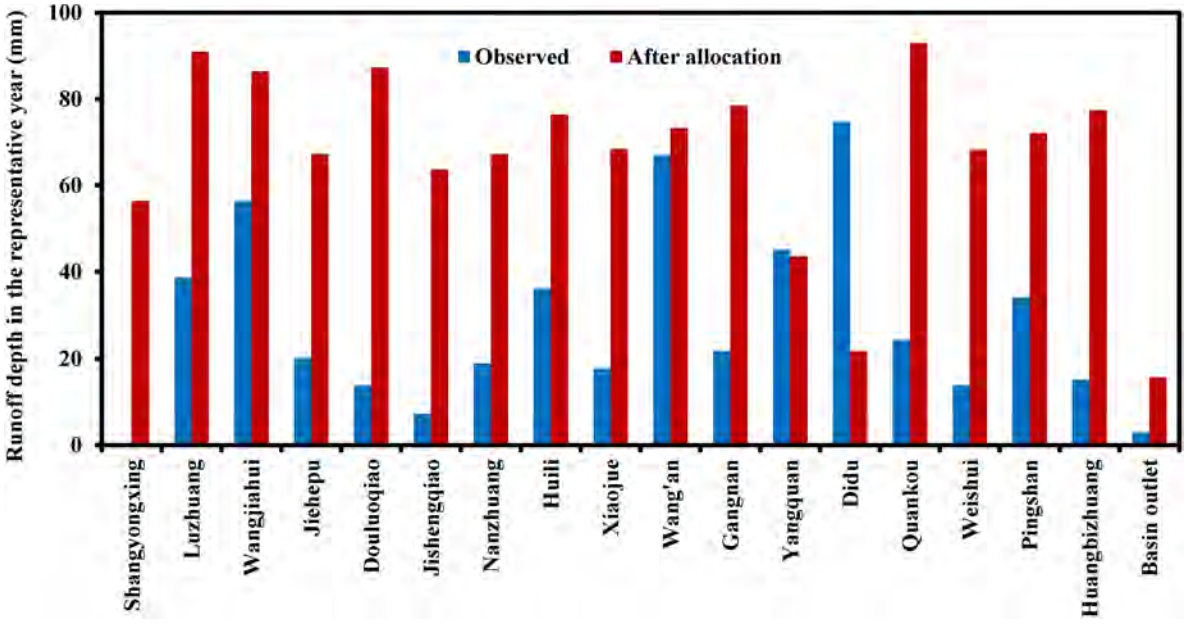

Fig. 8. Response of annual outlet runoff to agricultural water optimization in the representative year.

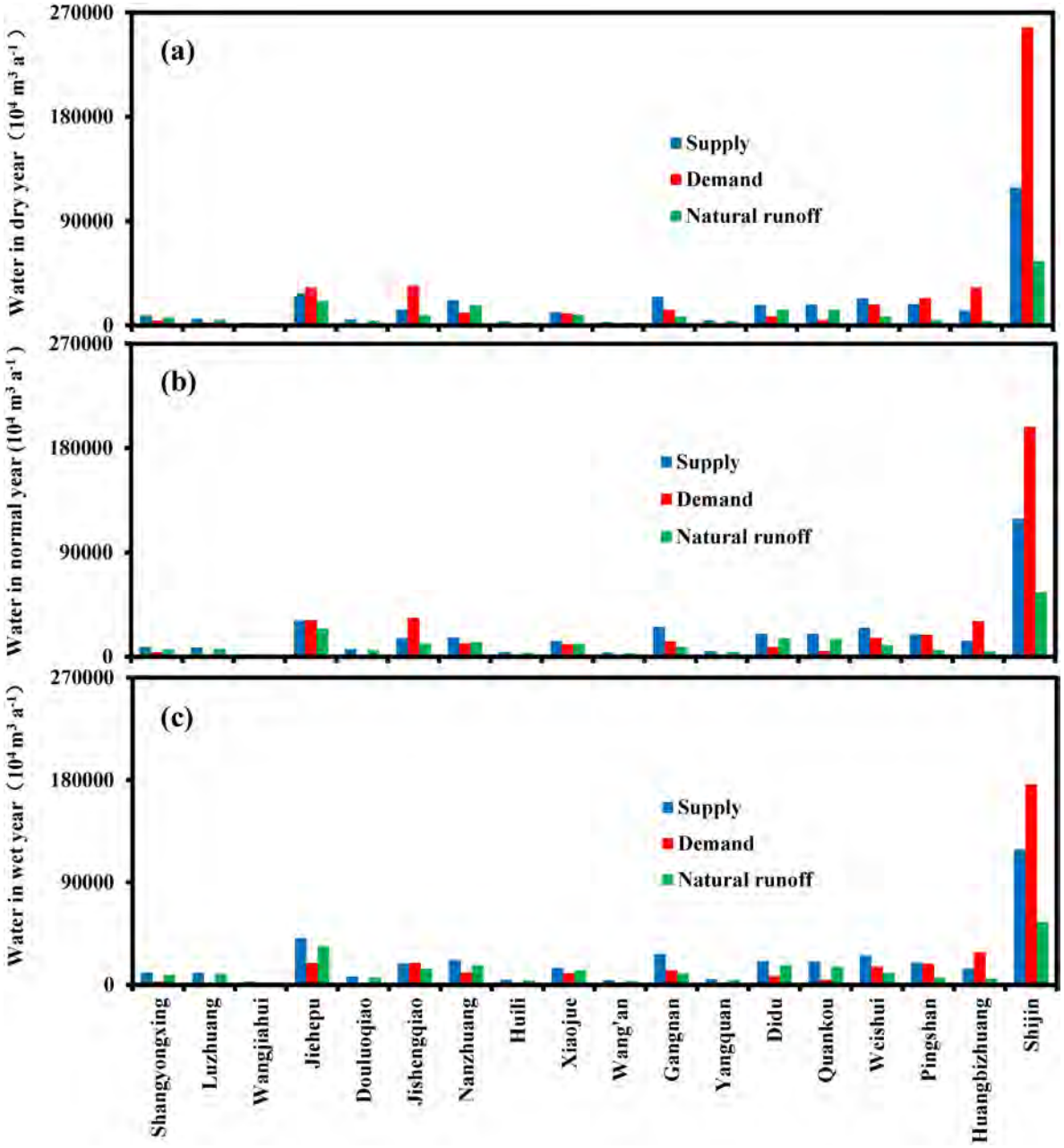

Fig. 9. Water supply and demand of each unit in different scenarios in 2020s. a, b and c is for the dry, normal and wet year, respectively.

are 0.82 and 0.75 in the calibration and validation periods respectively for Xiaojue (Fig. 6a), while 0.75 and 0.88 for Pingshan (Fig. 6b). The correlated coefficients are no less than 0.9 in both calibration and validation periods for these two sub-basins. According to Wang et al. (2013), the correlated coefficient is 0.93 in the calibration period and 0.79 in the validation period at Xiaojue for a two-parameter monthly hydrological model, while the Nash-Sutcliffe efficiency coefficient is 0.86 and 0.62, respectively. The difference of simulation efficiency between the calibration period and validation period of VIP model is lower than that in Wang et al. (2013), implying the robust performance of this distributed ecohydrological model in term of natural runoff reproduction.

The reproduced natural runoff is secondly evaluated in the representative year via the difference between water demand and water supply including the natural runoff (Fig. 7). Primarily, the calculated water demand is assessed. For units in Shanxi Province, the total water demand was about 6.41×10^8 m^3, which was larger than the reported value (6.05×10^8 m^3) in Shanxi water resources bulletin by 6%. Considering that the river ecological water demand of all units was calculated as the minimum natural monthly runoff in recent 10 years while in fact a few rivers dried up, the calculated water demand was acceptable. The water supply and demand for the whole basin was about 33.51×10^8 m^3 and 33.55×10^8m^3, with a difference of 0.12%. This indicates the reproduced natural runoff included in the water supply is effective.

4.3. Results of agricultural water optimization

After agricultural water optimization in the representative year (Table 5), the agricultural water for most units in the upper reach declines, particularly in the spring maize units with great rainfed yield (such as Jiehepu and Quankou unit) and winter wheat-summer maize

Table 6
Agricultural water optimization in 2020s.

	Normal year in 2020s						Dry year in 2020s				
	W_{c0}	W_{agr0}	X	Y	Y_0	Y_{opt}	W_{agr0}	X	Y	Y_0	Y_{opt}
Shangyongxing	72	1072	148	55	17,077	16,097	1300	150	57	14,547	11,141
Luzhuang	35	666	70	35	18,920	18,466	1171	127	35	13,573	11,386
Wangjiahui	2	906	93	2	15,253	14,592	792	113	2	8882	7002
Jiehepu	499	16,998	2029	188	290,394	275,333	17,987	2127	187	309,675	260,703
Douluoqiao	22	1116	137	22	28,305	27,661	1360	151	22	25,194	21,460
Jishengqiao	573	14,328	1829	214	326,512	317,059	3582	2142	573	300,201	295,640
Nanzhuang	73	1201	182	37	23,315	22,491	786	81	54	14,367	11,992
Huili	41	144	34	41	3937	3891	111	14	41	3369	2782
Xiaojue	92	579	88	64	14,361	14,067	339	36	86	10,015	8642
Yangquan	40	186	27	40	11,334	11,208	163	24	40	9969	9507
Didu	744	621	107	744	40,225	39,853	622	79	247	33,934	32,300
Quankou	160	933	142	160	82,487	81,811	913	132	105	67,309	64,342
Wang'an	8	655	80	8	14,144	10,389	838	102	8	19,577	10,366
Gangnan	19	2393	336	19	47,108	32,221	2593	368	19	63,801	34,134
Weishui	475	6541	809	433	139,660	122,275	8148	826	174	180,402	122,211
Pingshan	686	6351	788	242	171,964	147,707	10,295	1094	603	195,276	120,187
Huangbizhuang	408	8693	1087	408	195,767	141,157	10,555	1132	132	244,813	128,117
Shijin	4792	73,613	107,953	1554	3,688,599	3,947,911	49,369	107,008	1562	2,909,107	3,579,803

Notes: W_{c0} – annual urban ecological water demand (10^4 m^3), W_{agr0} – annual agricultural water without water optimization (10^4 m^3), X –agricultural water allocated to units (10^4 m^3), Y – urban ecological water allocated to units (10^4 m^3), Y_0 –crop yield without water optimization (ton), Y_{opt} –crop yield after water optimization (ton)

units with great actual irrigation water consumption (such as Pingshan and Huangbizhuang unit). Moreover, the urban ecological water in most units also decreases, particularly in the units with larger urban ecological water demand. These water decreases lead to a water increase of 0.74×10^8 m^3 in the lower reach. As a result, the water deficit in the lower reach decreases by 4%, and the crop yield in the lower reach increases by 0.44×10^8 kg (about 1.25%). For the whole basin, there is a yield increase of 0.19×10^8 kg (about 0.4%). Furthermore, the outflow of most units increases after agricultural water optimization, as well as the runoff into the sea (Fig. 8), which can effectively improve the ecology and environment of the basin.

In 2020s, there will be a water surplus of 5.79×10^8 m^3 (18%), water deficit of 3.09×10^8 m^3 (8%) and water deficit of 11.72×10^8 m^3 (26%) under the wet, normal and dry year scenario for the whole basin, respectively (Fig. 9). Under the wet year scenario, agricultural and urban ecological water of each unit will be fully satisfied, and the agricultural and ecological benefits will reach maximum value (100%). In addition, the difference of the agricultural water satisfaction ratio for all units will be the smallest. After agricultural water optimization under the normal and dry year scenarios (Table 6), the satisfaction ratio of urban ecological water for the whole basin can only reach 80% and 76%, the maximum satisfaction ratio of the agricultural water for the units in the upper reach will be about 23% and 14%, and the yield in irrigated farmlands for the whole basin can only reach 97% and 82% of that with sufficient irrigation, respectively. Due to water optimization, under the normal and dry year scenarios, the water supply from the upper reach to Shijin District will increase by 3.11×10^8 m^3 and 5.44×10^8 m^3, and the yield for the whole basin will increase by 1×10^8 kg (i.e. 2%) and 3×10^8 kg (i.e. 7%), respectively. Because the irrigation water use efficiency in the Shijin District is greater under the dry year scenario than that under the normal year scenario, the agricultural water optimization under the former scenario will be relatively more effective.

5. Discussion

5.1. Effects of spatial difference of natural runoff and crop photosynthetic capacity

The natural runoff takes up more than 60% of the water supply for the whole basin in all scenarios. The water resources allocated to agricultural and urban ecological sectors correlate significantly ($p < 0.01$, $r > 0.59$) with local natural runoff for all water units in the representative year, dry and normal year in 2020s. As the crop yield correlates significantly ($p < 0.01$, $r > 0.99$) with the allocated agricultural water, the local natural runoff can explain 49%, 63% and 62% ($p < 0.01$) of the crop yield for all units after water optimization in the representative year, dry and normal year in 2020s, respectively. Further, the local natural runoff can explain more than 45% ($p < 0.01$) of the outflow for the upper units in all these three scenarios. Overall, the spatial heterogeneity of natural runoff significantly impacts the agricultural production and outflow in water optimization.

The crop yield after water optimization is impacted by not only the allocated agricultural water but also the rainfed yield of irrigated farm ($p < 0.01$, $r > 0.99$). The rainfed yield per unit area in spring maize units correlates with the intrinsic quantum efficiency significantly ($r > 0.53$, $p < 0.05$) in the normal year in 2020s, but it is not significant in the representative or dry year in 2020s. It is because precipitation in the latter two scenarios is less and the crop yield correlates more closely with water. The rainfed yield per unit area in winter wheat-summer maize units can be explained more than 49% by the maximum catalytic capacity of Rubisco of winter wheat in all the representative year, dry and normal year in 2020s. Therefore, the effect of the spatial heterogeneity of crop photosynthetic capacity on agricultural production is essential in water optimization.

5.2. Uncertainty of parameters in the AWOMB

The weights of objective functions (Table 2) in this study are set according to the advice of experts, which is subjective. Taking the representative year as an example, we analyz the uncertainty of this method by fixing the weight of one objective function (Fig. 10). As a result, when the weight of agricultural benefit is fixed as 0.1, the agricultural benefit keeps as 0.75 (Fig. 10a). When the weight of social benefit is fixed as 0.1 (Fig. 10b), the agricultural benefit increases from 0.75 to 0.85 as the weight of agricultural benefit increases from 0 to 0.7, and the agricultural benefit almost keeps stable as the weight of agricultural benefit increases from 0.7 to 0.9. When the weight of ecological benefit is fixed as 0.1(Fig. 10c), the agricultural benefit increases from 0.75 to 0.85 as the weight of agricultural benefit increases from 0 to 0.5, and the agricultural benefit almost keeps stable as the weight of agricultural benefit increases from 0.5 to 0.9. These results

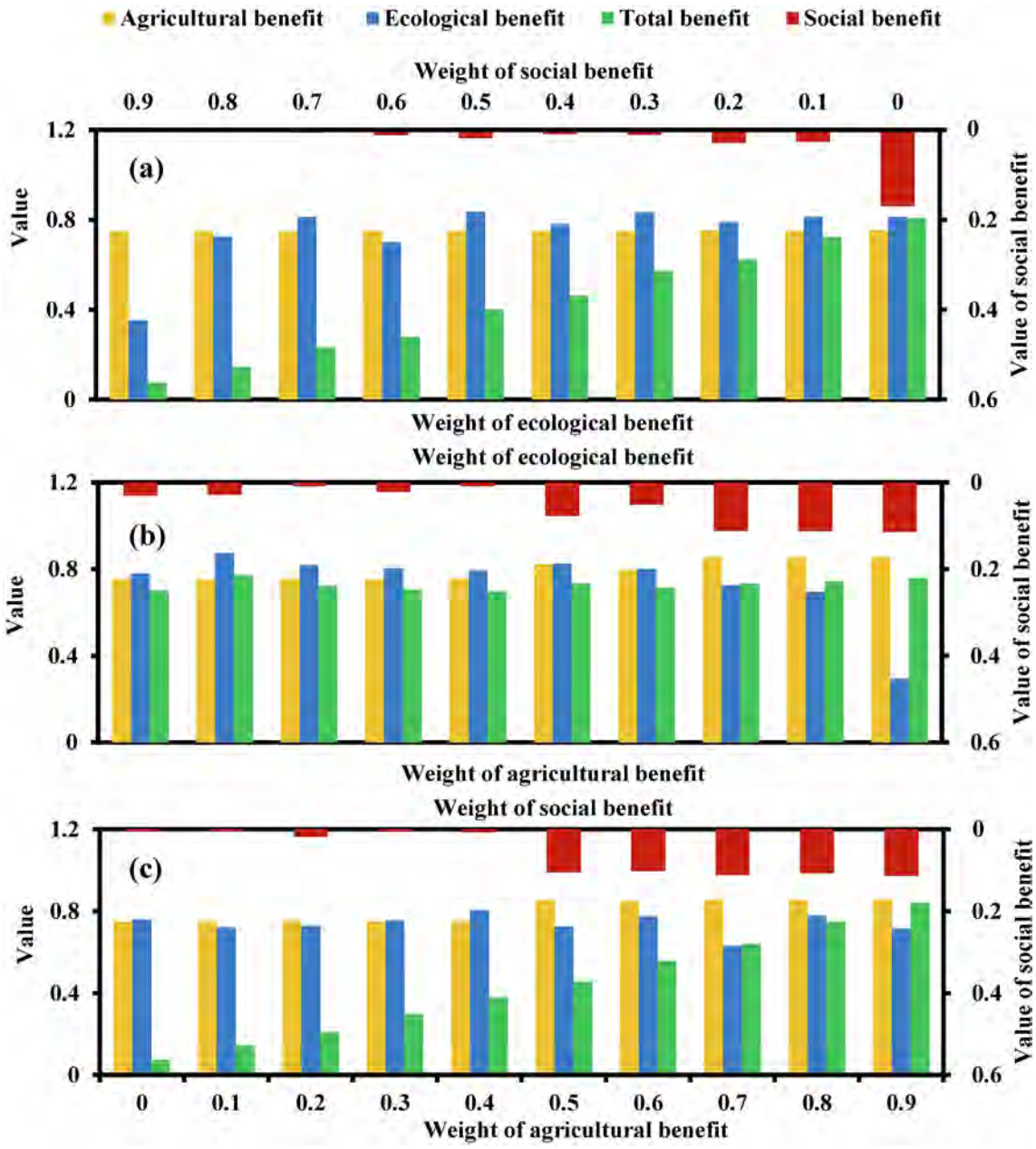

Fig. 10. Response of objective function values to the weights in the representative year. a, b, and c are set as a fixed weight (0.1) of agricultural, social and ecological benefit, respectively.

indicate that when the weight of agricultural benefit is no less than 0.7 (i.e. > 0.6), the optimal agricultural benefit can be obtained. When the weight of agricultural benefit increases from 0.7 to 0.9 (Fig. 10b and c), the agricultural and social benefits almost keep stable, and the ecological benefit reaches its relatively small value when the weight of agricultural benefit is 0.9 and 0.7 in Fig. 10b and Fig. 10c respectively. It implies the weight of agricultural benefit should be larger than 0.7 and smaller than 0.9. If the minimum increasing volume of weight is set as 0.1, the weight of agricultural benefit should be 0.8. The ecological and social benefits are considered equally important, their weights should be both 0.1. Therefore, the weights used in this work (0.8, 0.1 and 0.1 for the agricultural, ecological and social benefit, respectively) are valid.

The minimum satisfaction ratio of agricultural water (S_{amin}) and urban ecological water (S_{cmin}) is determined somewhat subjective (Table 2). In the representative year, we analyz the impact of these two parameters on agricultural water optimization (Fig. 11). It is found that when S_{amin} is fixed as any value ranging from 0.1 to 0.4, the ecological benefit increases significantly ($r > 0.83$, $p < 0.05$) as S_{cmin} increases from 0.1 to 1.0 (Fig. 11c), indicating the ecological benefit is sensitive to S_{cmin}. Further, the greater the S_{amin}, the smaller the increasing rate of ecological benefit resulting from S_{cmin} increase, implying the effect of S_{cmin} on ecological benefit decreases as S_{amin} increases. The reason is that when S_{amin} increases, the water allocated to ecology becomes less, which leads to smaller ecology benefit. Similarly, the social benefit (i.e. equity of agricultural water) is proved to be sensitive to S_{amin}, and the effect of S_{amin} on social benefit decreases as S_{cmin} increases. Moreover, as S_{amin} or S_{cmin} changes, the variances of ecological and social benefits are about 0.1 (Fig. 11c, d), and that of the agricultural benefit is about 0.01 (Fig. 11b). Due to the weights of the former two are both small and that of the latter one is great, the variance of total benefit is also about 0.01 (Fig. 11a). It shows that the uncertainty of S_{amin} and S_{cmin} is limited. In addition, when S_{amin} and S_{cmin} are 0.1 and 0.3 respectively (Table 2), the value of the main objective function (i.e. agricultural

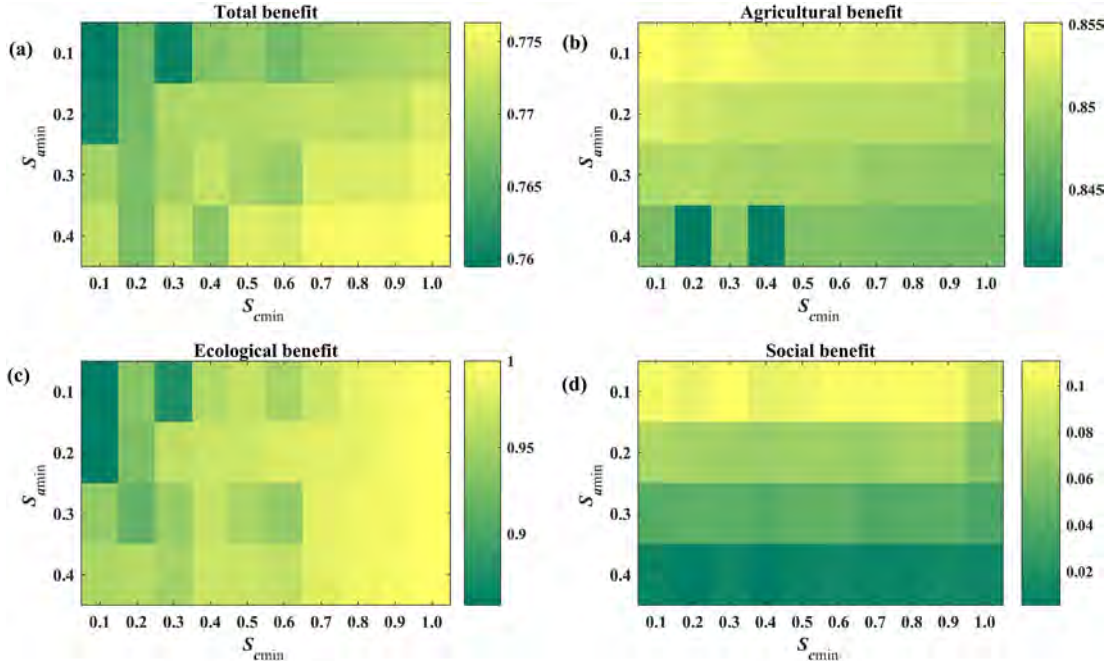

Fig. 11. Response of objective function values to the minimum satisfaction ratio of agricultural and urban ecological water demand. S_{amin} and S_{cmin} is the minimum satisfaction ratio of agricultural and urban ecological water, respectively. (a)-Total benefit, (b)-Agricultural benefit, (c)-Ecological benefit, and (d)-Social benefit.

benefit) is relatively great (Fig. 11b). Thus, the values of S_{amin} and S_{cmin} in this work are rational.

5.3. Implications and limitations

The results show that the developed agricultural water optimization scheme involving the spatial heterogeneity of crop photosynthetic capacity and natural runoff is effective at the basin scale. However, there are some limitations of our agricultural water optimization scheme. First, the distributed ecohydrological model is coupled in agricultural water optimization via providing data, which cannot completely reflect the dynamic agro-hydrological process at the basin scale. Second, CWPF is constructed for the whole growing season due to the shortage of seasonal photosynthetic capacity parameters, which cannot reflect the impacts of irrigation at different growth stages on crop yield. However, the effect of irrigation depends on the particular growth stage (Singh et al., 1991). For example, water restriction has the greatest negative effects on maize grain production during or after silking by reducing the number of kernels and limiting kernel filling (Soderlund et al., 2014). Third, three years with different annual precipitation are chosen to demonstrate different water resource scenarios in 2020s, which is limited in water optimization at the monthly scale. Last but not least, the agricultural water in this work is a rough estimate since the detailed map of crop pattern is not available.

The developed agricultural water optimization model with VIP model is appropriate for water resources planning in a river basin where human activities (such as irrigation) have great impact on the discharge or crop yield, particular the latter due to that the response of crop yield to crop photosynthetic capacity heterogeneity can be efficiently reproduced with VIP model. The spatial pattern of crop photosynthetic capacity parameter is the prime requirement to extend the developed AWOMB in other areas. More, information regarding the groundwater, other water resources, domestic water demand, industrial water demand, urban ecological water demand and the spatial distribution of irrigated farm is required for water demand calculation. This work also provides a pragmatic methodology to employ the distributed model to manage water resources at the basin scale, which is accomplished by providing CWPFs involving the spatial heterogeneity of sensitive crop yield parameter and runoff of sub-basins.

6. Conclusions

In order to improve the water utilization and agricultural production in a basin with intensive irrigation, the AWOMB was developed with the help of a distributed ecohydrological model (VIP model). Namely, the CWPF in the AWOMB accounting for the spatial heterogeneity of the effect of photosynthetic capacity on irrigation water productivity was obtained with VIP model, as well as the natural runoff of sub-basins. After evaluation of CWPF and natural runoff, agricultural water optimization was conducted under different scenarios, and the response of crop yield and outflow was analyzed.

The irrigation water calculated with CWPF considering the spatial heterogeneity of crop photosynthetic capacity reproduced the actual volume well. The variables used in this kind of CWPF were rational under different scenarios. The generated natural runoff of different sub-basins agreed with the observed value and was effective in the water balance equation. The agricultural water optimization method involving the spatial heterogeneity of crop photosynthetic capacity and natural runoff can be used to manage agricultural water at the basin scale.

The local natural runoff dominated the water allocation to the water units in the agricultural water optimization at the basin scale. In the representative year, the optimal agricultural water allocation scheme not only enhanced the agricultural benefit but also improved the river ecological water and the runoff into the sea. After agricultural water optimization, due to agricultural water decrease in the upper sub-basins where rainfed crop yield or actual irrigation water was high, the water supply in the lower reach with great potential crop productivity increased by 5%, resulting in a crop yield increase of 0.19×10^8 kg for the whole basin. However, some urban ecological water and equity of agricultural water was sacrificed.

In 2020s, there will be a water surplus for the whole basin under the wet year scenario, and the crop yield will reach the yield with sufficient irrigation. Under the normal and dry year scenarios, there will be water deficits for the whole basin. In order to guarantee crop yield, the water supply from the upper reach to the lower reach should increase. In the dry and normal year scenarios, if the water supply from the upper reach to the lower reach increases by 5.44×10^8 m^3 and 3.11×10^8, the yield in the lower reach will increase by 3×10^8 kg (7%) and 1×10^8 kg (i.e. 2%), respectively. Further, the effect of spatial heterogeneity of crop photosynthetic capacity on agricultural production will be particularly important in the normal year scenario.

With the distributed ecohydrological model, a practical agricultural water optimization model is constructed for the whole basin at the annual scale. This technique can be used for water resource planning in a river basin.

Declaration of Competing Interest

The authors declare that they have no known competing financial interests or personal relationships that could have appeared to influence the work reported in this paper.

Acknowledgements

This research was supported by the National Natural Science Foundation of China (Grant No. 41471026, 41790424). The authors thank Dr. L. X. LI from Ontario Veterinary Medical Association for her linguistic assistance of this manuscript. The authors appreciate the editor and the two anonymous reviewers for their efforts and constructive comments on the manuscript.

Appendix A:. The natural runoff reproduction in the upstream units

Since the streamflow in the upper reach changed abruptly around 1979 (Yang and Tian, 2009; Huang and Mo, 2015), the period from 1956 to 2013 was separated into the base period (1956–1979) and changing period (1980–2013). In the base period, the effect of human activities on the streamflow could be neglected, thus the observed streamflow was considered as the natural streamflow. In the changing period, the effect of human activities was significant, and the observed streamflow was impacted by human activities, such as irrigation. With the natural streamflow in the base period, VIP model can be calibrated and validated to simulate the natural runoff. With the calibrated parameters, the natural runoff of sub-basins in the changing period can be reproduced. For the unit which is a separate sub-basin, the annual natural runoff R_{nkt} (m^3) is taken as the natural runoff simulated by VIP model. For the unit which is not a separate sub-basin, R_{nkt} is derived according to the hydrographic net:

$$R_{nkt} = R_{nkt\_basin} - \sum_{k=k_0}^{k=k_1} R_{nkt\_sub} \tag{A1}$$

Here, R_{nkt_basin} (m^3) is the reproduced natural runoff in year t of the sub-basin (*k_basin*) that unit k is included, R_{nkt_sub} (m^3) is the value of separate sub-basin (*k_sub*) included in *k_basin*, k_0 and k_1 are the first and last number for *k_sub*.

Appendix B:. Water demand calculation

(1) In year t , the domestic water demand of unit k W_{lifekt} (m^3) is given by:

$$W_{lifekt} = W_{citykt} + W_{ruralkt} \tag{B1}$$

$$W_{citykt} = \frac{P_{citykt} \times K_{citykt} \times n_{dayt}}{1000} \tag{B2}$$

$$W_{ruralkt} = \frac{P_{ruralkt} \times K_{ruralkt} \times n_{dayt}}{1000} \tag{B3}$$

where W_{citykt} and $W_{ruralkt}$ are the annual urban and rural domestic water demand in year t (m^3), K_{citykt} and $K_{ruralkt}$ are the urban and rural domestic water quota (L $day^{-1}person^{-1}$) (Tables 1 and 3), respectively. n_{dayt} is the total days in year t. P_{citykt} and $P_{ruralkt}$ are the urban and rural population respectively, and the former is calculated with the total population P_{kt} and the urbanization rate U_{kt} (Tables 1 and 3). P_{kt} is expressed as:

$$P_{kt} = P_{citykt} + P_{ruralkt} = P_{kt} \times U_{kt} + P_{ruralkt} = P_{ok} \times (1 \pm v_k)^n \tag{B4}$$

Here n is the number of years for prediction, P_{ok} is the population in a given year, derived from the spatial distribution of population in 2010 (Fu et al., 2014), and v_k is the natural population growth rate (Table 1) obtained from the statistical data.

(2) In unit k in year t, the industrial water demand W_{indkt} (m^3) is inferred as:

$$W_{indkt} = GDP_{indkt} \times Q_{indkt} \times (1 - \eta_{indkt}) \tag{B5}$$

Here Q_{indkt} is the water consumption per 10^4 Yuan GDP (m^3 $(10^4 Yuan)^{-1}$) (Tables 1 and 3), and η_{indkt} is the reuse rate of industrial water from the reported data (Table 1). GDP_{indkt} is the industrial GDP in unit k in year t (10^4Yuan), predicted by the following equation,

$$GDP_{indkt} = GDP_{indok} \times (1 \pm vi)^n \tag{B6}$$

n is the number of years for prediction, GDP_{indok} (10^4Yuan) is the industrial GDP in a given year, derived from the spatial distribution of GDP in 2010 and the relationship between GDP and land use types (Huang et al., 2014a, 2014b), and vi (10^4Yuan $year^{-1}$) is the averaged growth rate of industrial GDP (Table 1).

(3) In year t, the river ecological water demand of unit k W_{rkt} (m^3) refers to the minimum streamflow to maintain the survival of aquatic and riparian life, which is calculated as the minimum natural monthly runoff in 2004–2013 based on the 7Q10 method (DFID of the UK, 2003). The natural monthly runoff is reproduced by VIP model (Appendix A).

The urban ecological water demand of unit k W_{ckt} (m^3) is given by:

$$W_{ckt} = P_{citykt} \times q_n \tag{B7}$$

Here q_n is the urban ecological water quota. The recommended value of q_n is 20 m^3 $year^{-1}$ $person^{-1}$ (Fu, 2012).

(4) The upper bound of the agricultural water is the maximum irrigation water W_{agrskt} (m^3), given by:

$$W_{agrskt} = \frac{I_{skt} \times I_{ak}}{10 \times \alpha_{kt}} \tag{B8}$$

where α_{kt} is the effective irrigation water utilization rate (Tables 1 and 3), referring to the ratio of water stored in the root zone to the water withdrawal in the water source. I_{skt} (mm) is the annual sufficient irrigation per unit area (average value for unit k), simulated by VIP model (Section 3.3). I_{ak} (ha) is the irrigated area of unit k (Fig. 3a), calculated based on the spatial distribution of irrigated farm (Fig. 1b). The irrigated farm grid is identified by the NDVI threshold method. Namely, the multi-year (2005-2013) mean accumulated NDVI from April to September of all farm grids (at a spatial resolution of 250 m) is descending sorted; if the irrigation ratio of the region is about 30%, NDVI threshold is the NDVI with 30% percentile. The farm grids with NDVI larger than the threshold belong to irrigated farm.

The gross actual agricultural water W_{agrakt} (m^3) is expressed as:

$$W_{agrakt} = \frac{I_{Rkt} \times I_{ak}}{10 \times \alpha_{kt}} \tag{B9}$$

where I_{Rkt} (mm) is the annual actual irrigation per unit area (average value for unit k), derived from the following equation:

$$I_R = \begin{cases} ET_a - P_{valid} & ET_a \geqslant P_{valid} \\ 0 & ET_a < P_{valid} \end{cases} \tag{B10}$$

Because the cycle of soil water is about one year, ET_a is the annual actual ET (mm), which is derived based on remote sensing NDVI at the spatial resolution of 250 m (Mo et al., 2015). P_{valid} is the effective precipitation in the corresponding period (mm), calculated with the method recommended by the soil and water conservation bureau of the United States Department of Agriculture:

$$P_{eff} = \begin{cases} P_{month} \times (125 - 0.2 \times P_{month})/125 & P_{month} \leqslant 250mm \\ 125 + 0.1 \times P_{month} & P_{month} > 250mm \end{cases} \tag{B11}$$

Here P_{eff} is the effective monthly precipitation (mm $month^{-1}$), and P_{month} is the monthly precipitation (mm $month^{-1}$).

References

Ahrends, H., Mast, M., Rodgers, C., Kunstmann, H., 2008. Coupled hydrological-economic modelling for optimised irrigated cultivation in a semi-arid catchment of West Africa. Environ. Modell. Software 23 (4), 385–395. https://doi.org/10.1016/j.envsoft.2007.08.002.

Alvarez, J.F.O., Valero, J.A.D., Martin-Benito, J.M.T., Mata, E.L., 2004. MOPECO: an economic optimization model for irrigation water management. Irrig. Sci. 23 (2), 61–75. https://doi.org/10.1007/s00271-004-0094-x.

Ball, J.T., Woodrow, I., Berry, J.A., 1987. A model predicting stomatal conductance and its contribution to the control of photosynthesis under different environmental conditions. Prog. Photosynth. Res. 4, 221–224.

Bos, M.G., 1980. Irrigation efficiencies at crop production level. ICID Bull. 29, 18–25.

Bos, M.G., 1985. Summary of ICID definitions of irrigation efficiency. ICID Bull. 34, 28–31.

Brauman, K.A., Siebert, S., Foley, J.A., 2013. Improvements in crop water productivity increase water sustainability and food security-a global analysis. Environ. Res. Lett. 8 (2). https://doi.org/10.1088/1748-9326/8/2/024030.

Brück, H., Guo, S., 2006. Influence of N form on growth photosynthesis of Phaseolus vulgaris L. plants. J. Plant Nutr. Soil Sci. 169 (6), 849–856. https://doi.org/10.1002/jpln.200520570.

Cai, X.M., 1999. A modeling framework for sustainable water resources management. The University of Texas at Austin, Austin.

Cai, X.M., McKinney, D.C., Lasdon, L.S., 2002. A framework for sustainability analysis in water resources management and application to the Syr Darya Basin. Water Resour. Res. 38 (6). https://doi.org/10.1029/2001wr000214.

Collatz, G., Ribas-Carbo, M., Berry, J., 1992. Coupled Photosynthesis-Stomatal Conductance Model for Leaves of C4 Plants. Funct. Plant Biol. 19 (5), 519–538. https://doi.org/10.1071/PP9920519.

Dai, C., Qin, X.S., Chen, Y., Guo, H.C., 2018. Dealing with equality and benefit for water allocation in a lake watershed: A Gini-coefficient based stochastic optimization approach. J. Hydrol. 561, 322–334. https://doi.org/10.1016/j.jhydrol.2018.04.012.

Dang, T., Pedroso, R., Laux, P., Kunstmann, H., 2018. Development of an integrated hydrological-irrigation optimization modeling system for a typical rice irrigation scheme in Central Vietnam. Agric. Water Manag. 208, 193–203. https://doi.org/10.1016/j.agwat.2018.05.018.

Deng, X.P., Shan, L., Zhang, H.P., Turner, N.C., 2006. Improving agricultural water use efficiency in arid and semiarid areas of China. Agric. Water Manage 80 (1–3), 23–40. https://doi.org/10.1016/j.agwat.2005.07.021.

DFID of the UK, 2003. Handbook for the assessment of catchment water demand and use. HR Wallingford, Oxon, pp. 20–41.

Dong, C., Huang, G., Cheng, G., Zhao, S., 2018. Water Resources and Farmland Management in the Songhua River Watershed under Interval and Fuzzy Uncertainties. Water Resour. Manage. 32 (13), 4177–4200. https://doi.org/10.1007/s11269-018-2035-0.

Farquhar, G.D., von Caemmerer, S., Berry, J.A., 1980. A biochemical model of photosynthetic CO2 assimilation in leaves of C3 species. Planta 149 (1), 78–90. https://doi.org/10.1007/BF00386231.

Fu, C.F., 2012. Research and application on ecology and plan mathematic model for water resources of Ziyahe Drainage Area. Tianjin University, Tianjin.

Fu, J.Y., Jiang, D., Huang, Y.H., 2014. PopulationGrid_China. Global Change Research Data Publishing and Repository.

Fu, J., Zhong, P., Chen, J., Xu, B., Zhu, F., Zhang, Y., 2019. Water Resources Allocation in Transboundary River Basins Based on a Game Model Considering Inflow Forecasting Errors. Water Resour. Manage. 33 (8), 2809–2825. https://doi.org/10.1007/s11269-019-02259-y.

Galán-Martín, Á., Vaskan, P., Antón, A., Esteller, L.J., Gonzalo, G., 2017. Multi-objective optimization of rained and irrigated agricultural areas considering production and environmental criteria: a case study of wheat production in Spain. J. Cleaner Prod. 140, 816. https://doi.org/10.1016/j.jclepro. 2016.06.099.

Garcia-Vila, M., Fereres, E., 2012. Combining the simulation crop model AquaCrop with an economic model for the optimization of irrigation management at farm level. Eur. J. Agron. 36 (1), 21–31. https://doi.org/10.1016/j.eja.2011.08.003.

Garg, N.K., Dadhich, S.M., 2014. Integrated non-linear model for optimal cropping pattern and irrigation scheduling under deficit irrigation. Agric. Water Manage. 140, 1–13. https://doi.org/10.1016/j.agwat.2014.03.008.

Goldberg, D.E., 1989. Genetic Algorithms in Search. Optimization and Machine Learning, Addision-Wesley, Reading, MA.

Guo, Y., Shen, Y., 2015. Quantifying water and energy budgets and the impacts of climatic and human factors in the Haihe River Basin, China: 2. Trends and implications to water resources. J. Hydrol. 527, 251–261. https://doi.org/10.1016/j.jhydrol.2015.04.071.

Hasson, S.u., Saeed, F., Böhner, J., Schleussner, C.F., 2019. Water availability in Pakistan from Hindukush–Karakoram–Himalayan watersheds at 1.5 °C and 2 °C Paris Agreement targets. Adv. Water Resour. 131, 103365. https://doi.org/10.1016/j.advwatres.2019.06.010.

Hu, S., Mo, X., 2011. Interpreting spatial heterogeneity of crop yield with a process model and remote sensing. Ecol. Model. 222 (14), 2530–2541. https://doi.org/10.1016/j.ecolmodel.2010.11.011.

Hu, S., Mo, X., Huang, F., 2019. Retrieval of photosynthetic capability for yield gap attribution in maize via model-data fusion. Agric. Water Manage. 226, 105783. https://doi.org/10.1016/j.agwat.2019.105783.

Hu, S., Mo, X., Lin, Z., 2014. Optimizing the photosynthetic parameter V-cmax by assimilating MODIS-f(PAR) and MODIS-NDVI with a process-based ecosystem model. Agric. For. Meteorol. 198, 320–334. https://doi.org/10.1016/j.agrformet.2014.09.002.

Hu, S., Mo, X., Lin, Z., Qiu, J., 2010. Emergy assessment of a wheat-maize rotation system with different water assignments in the north China plain. Environ. Manage. 46 (4), 643–657. https://doi.org/10.1007/s00267-010-9543-x.

Huang, F., Mo, X., 2015. Water budget and its variation in Hutuo River basin predicted with the VIP ecohydrological model. In: Chen, Y. (Ed.), Remote Sensing and Gis for Hydrology and Water Resources. IAHS Publication, pp. 460–465.

Huang, Y.H., Jiang, D., Fu, J.Y., 2014a. GDPGrid_China. Acta Geographica Sinica 69 (supplement), 45–48.

Huang, Y. H., Jiang, D., Fu, J. Y., 2014b. GDPGrid_China. Global Change Research Data Publishing and Repository. http://www.geodoi.ac.cn/doi.aspx?doi=10.3974/geodb.2014. 01.07.v1.

Jiang, Y., Xu, X., Huang, Q., Huo, Z., Huang, G., 2015. Assessment of irrigation performance and water productivity in irrigated areas of the middle Heihe River basin using a distributed agro-hydrological model. Agric. Water Manage. 147, 67–81. https://doi.org/10.1016/j.agwat.2014.08.003.

Jiang, Y., Xu, X., Huang, Q., Huo, Z., Huang, G., 2016. Optimizing regional irrigation water use by integrating a two-level optimization model and an agro-hydrological model. Agric. Water Manage. 178, 76–88. https://doi.org/10.1016/j.agwat.2016.08.035.

Kendy, E., Gerard-Marchant, P., Walter, M.T., Zhang, Y.Q., Liu, C.M., Steenhuis, T.S., 2003. A soil-water-balance approach to quantify groundwater recharge from irrigated cropland in the North China Plain. Hydrol. Process. 17 (10), 2011–2031. https://doi.org/10.1002/hyp.1240.

Li, D., Du, T., Sun, Q., Cao, Y., 2019a. The key driving factors of irrigation water productivity based on soil spatio-temporal characteristics. Agric. Water Manage. 216, 351–360. https://doi.org/10.1016/j.agwat.2019. 01.027.

Li, K., Huang, G., Wang, S., 2019b. Market-based stochastic optimization of water resources systems for improving drought resilience and economic efficiency in arid regions. J. Cleaner Prod. 233, 522–537. https://doi.org/10.1016/j.jclepro.2019.05.379.

Li, M., Xu, Y., Fu, Q., Singh, V.P., Liu, D., Li, T., 2020a. Efficient irrigation water allocation and its impact on agricultural sustainability and water scarcity under uncertainty. J. Hydrol. https://doi.org/10.1016/j.jhydrol.2020.124888.

Li, X., Zhang, C., Huo, Z., 2020b. Optimizing irrigation and drainage by considering agricultural hydrological process in arid farmland with shallow groundwater. J. Hydrol. https://doi.org/10.1016/j.jhydrol.2020.124785.

Li, Y.Z., Xu, G.M., Lv, K.J., 2007. Water resources optimized allocation of Shijiazhuang after South-to-North Water Diversion. Water Saving Irrigation 8, 55–57.

Lin, Z.H., 2003. Spatial simulation of summer maize yield and water use efficiency using GIS and RS based crop growth model. Institute of Geographic Science and Natural Resources Research, Chinese Academy of Sciences, Beijing.

Lin, Z., Mo, X., Li, H., Li, H., 2002. Comparison of three spatial interpolation methods for climate variables in china. Acta Geographica Sinica 57 (1), 47–56.

Linker, R., 2020. Unified framework for model-based optimal allocation of crop areas and water. Agric. Water Manag. 228, 105859. https://doi.org/10.1016/j.agwat.2019.105859.

Liu, B., Chen, X., Meng, Q., Yang, H., van Wart, J., 2017. Estimating maize yield potential and yield gap with agro-climatic zones in China Distinguish irrigated and rainfed conditions. Agric. For. Meteorol. 239, 108–117. https://doi.org/10.1016/j.agrformet.2017.02.035.

Liu, D., Tian, F., Lin, M., Sivapalan, M., 2015. A conceptual socio-hydrological model of the co-evolution of humans and water: case study of the Tarim River basin, western China. Hydrol. Earth Syst. Sci. 19 (2), 1035–1054. https://doi.org/10.5194/hess-19-1035-2015.

Ma, L., Yang, Y., Yang, Y., Xiao, D., Bi, S., 2011. The distribution and driving factors of irrigation water requirements in the North China Plain. Journal of Remote Sensing 15 (2), 324–339.

Mekonnen, D.K., Channa, H., Ringler, C., 2015. The impact of water users' associations on the productivity of irrigated agriculture in Pakistani Punjab. Water Int. 40 (5–6), 733–747. https://doi.org/10.1080/02508060.2015.1094617.

Meng, Q., Chen, X., Lobell, D.B., Cui, Z., Zhang, Y., Yang, H., Zhang, F., 2016. Growing sensitivity of maize to water scarcity under climate change. Sci. Rep. 6. https://doi.org/10.1038/srep19605.

Michalewicz, Z., 1994. Genetic Algorithms + Data Structures = Evolution Programs. Spring, Berlin.

Mo, X., Beven, K.J., Liu, S., Leslie, L.M., De Roo, A.P.J., 2005a. Long-term water budget estimation with the modified distributed model – LISFLOOD-WB over the Lushi basin. China. Meteorology and Atmospheric Physics 90 (1–2), 1–16. https://doi.org/10.1007/s00703-004-0084-9.

Mo, X., Chen, X., Hu, S., Liu, S., Xia, J., 2017. Attributing regional trends of evapotranspiration and gross primary productivity with remote sensing: a case study in the North China Plain. Hydrol. Earth Syst. Sci. 21 (1), 295–310. https://doi.org/10.5194/hess-21-295-2017.

Mo, X., Liu, S., Chen, X., Hu, S., 2018. Variability, tendencies, and climate controls of terrestrial evapotranspiration and gross primary productivity in the recent decade over China. Ecohydrology 11 (4), e1951. https://doi.org/10.1002/eco.1951.

Mo, X., Liu, S., Lin, Z., Guo, R., 2009. Regional crop yield, water consumption and water use efficiency and their responses to climate change in the North China Plain. Agric. Ecosyst. Environ. 134 (1–2), 67–78. https://doi.org/10.1016/j.agee.2009.05.017.

Mo, X., Liu, S., Lin, Z., Wang, S., Hu, S., 2015. Trends in land surface evapotranspiration across China with remotely sensed NDVI and climatological data for 1981–2010. Hydrological Sciences Journal-Journal Des Sciences Hydrologiques 60 (12), 2163–2177. https://doi.org/10.1080/02626667.2014.950579.

Mo, X.G., Liu, S.X., Lin, Z.H., Xu, Y.Q., Xiang, Y., McVicar, T.R., 2005b. Prediction of crop yield, water consumption and water use efficiency with a SVAT-crop growth model using remotely sensed data on the North China Plain. Ecol. Model. 183 (2–3), 301–322. https://doi.org/10.1016/j.ecolmodel. 2004.07.032.

Montesinos, P., Camacho, E., Alvarez, S., 2001. Seasonal furrow irrigation model with genetic algorithms (OPTIMEC). Agric. Water Manag. 52 (1), 1–16. https://doi.org/10.1016/s0378-3774(01)00129-9.

Nguyen, D.C.H., Ascough, J.C., Maier, H.R., Dandy, G.C., Andales, A.A., 2017. Optimization of irrigation scheduling using ant colony algorithms and an advanced cropping system model. Environ. Modell. Software 97, 32–45. https://doi.org/10.1016/j.envsoft.2017.07.002.

Potopova, V., Stepanek, P., Mozny, M., Tuerkott, L., Soukup, J., 2015. Performance of the standardised precipitation evapotranspiration index at various lags for agricultural drought risk assessment in the Czech Republic. Agric. For. Meteorol. 202, 26–38. https://doi.org/10.1016/j.agrformet.2014.11.022.

Sadeghi, S.H., Sharifi Moghadam, E., Delavar, M., Zarghami, M., 2020. Application of water-energy-food nexus approach for designating optimal agricultural management pattern at a watershed scale. Agric. Water Manag. 233, 106071. https://doi.org/10.1016/j.agwat.2020.106071.

Saseendran, S.A., Ahuja, L.R., Ma, L., Trout, T.J., McMaster, G.S., Nielsen, D.C., Ham, J.M., Andales, A.A., Halvorson, A.D., Chavez, J.L., Fang, Q.X., 2015. Developing and normalizing average corn crop water production functions across years and locations using a system model. Agric. Water Manage. 157, 65–77. https://doi.org/10.1016/j.agwat.2014.09.002.

Savitzky, A., Golay, M.J.E., 1964. smoothing Smoothing and differentiation of data by simplified least squares procedures. Anal. Chem. 36 (8), 1627–1639. https://doi.org/10.1021/ac60214a047.

Schlager, E., 2005. Rivers for Life: Managing water for people and nature. Ecol. Econ. 55 (2), 306–307. https://doi.org/10.1016/j.ecolecon.2005.08.004.

Siddiqi, A., Wescoat Jr., J.L., 2013. Energy use in large-scale irrigated agriculture in the Punjab province of Pakistan. Water Int. 38 (5), 571–586. https://doi.org/10.1080/02508060.2013.828671.

Singh, A., 2012. An overview of the optimization modelling applications. J. Hydrol. 466–467, 167–182. https://doi.org/10.1016/j.jhydrol.2012.08.004.

Singh, P.K., Mishra, A.K., Imtiyaz, M., 1991. Moisture stress and the water-use efficiency of mustard. Agric. Water Manage. 20 (3), 245–253. https://doi.org/10.1016/0378-3774(91)90021-a.

Singh, R., Jhorar, R.K., van Dam, J.C., Feddes, R.A., 2006. Distributed ecohydrological modelling to evaluate irrigation system performance in Sirsa district, India II: Impact of viable water management scenarios. J. Hydrol. 329, 714–723. https://doi.org/10.1016/j.jhydrol.2006.03.016.

Smilovic, M., Gleeson, T., Adamowski, J., Langhorn, C., 2019. More food with less water - Optimizing agricultural water use. Adv. Water Resour. 123, 256–261. https://doi.org/10.1016/j.advwatres.2018.09.016.

Soderlund, S., Owens, F.N., Fagan, C., 2014. Development of and field experience with drought-tolerant maize. J. Anim. Sci. 92 (7), 2823–2831. https://doi.org/10.2527/jas.2013-7373.

Su, X., Li, J., Singh, V.P., 2014. Optimal allocation of agricultural water resources based on virtual water subdivision in Shiyang River Basin. Water Resour. Manage. 28 (8), 2243–2257. https://doi.org/10.1007/s11269-014-0611-5.

Sun, H., Shen, Y., Yu, Q., Flerchinger, G.N., Zhang, Y., Liu, C., Zhang, X., 2010. Effect of precipitation change on water balance and WUE of the winter wheat-summer maize rotation in the North China Plain. Agric. Water Manage. 97 (8), 1139–1145. https://doi.org/10.1016/j.agwat.2009.06.004.

Tan, Q., Zhang, T., 2018. Robust fractional programming approach for improving agricultural water-use efficiency under uncertainty. J. Hydrol. 564, 1110–1119. https://doi.org/10.1016/j.jhydrol. 2018.07.080.

Vicente-Serrano, S.M., Peña-Gallardo, M., Hannaford, J., Murphy, C., Lorenzo-Lacruz, J., Dominguez-Castro, F., López-Moreno, J., Begueria, S., Noguera, I., Harrigan, S., Vidal, J.P., 2019. Climate, irrigation, and land-cover change explain streamflow trends in countries bordering the Northeast Atlantic. Geophys. Res. Lett. https://doi.org/10.1029/2019gl084084.

Wang, S., Huang, G.H., 2015. A multi-level Taguchi-factorial two-stage stochastic programming approach for characterization of parameter uncertainties and their interactions: An application to water resources management. Eur. J. Oper. Res. 240 (2), 572–581. https://doi.org/10.1016/j.ejor.2014.07.011.

Wang, S., Liu, S., Mo, X., Peng, B., Qiu, J., Li, M., Liu, C., Wang, Z., Bauer-Gottwein, P., 2015. Evaluation of Remotely Sensed Precipitation and Its Performance for Streamflow Simulations in Basins of the Southeast Tibetan Plateau. J. Hydrometeorol. 16 (6), 2577–2594. https://doi.org/10.1175/jhm-d-14-0166.1.

Wang, W., Shao, Q., Yang, T., Peng, S., Xing, W., Sun, F., Luo, Y., 2013. Quantitative assessment of the impact of climate variability and human activities on runoff changes: a case study in four catchments of the Haihe River basin, China. Hydrol. Process. 27 (8), 1158–1174. https://doi.org/10.1002/hyp.9299.

Wang, Z.G., Zhu, X.J., Xia, J., Li, J.X., 2008. Study on distributed hydrological model in Hai River Basin. Progress in Geography 27 (4), 1–6.

Wen, Y., Shang, S., Yang, J., 2017. Optimization of irrigation scheduling for spring wheat with mulching and limited irrigation water in an arid climate. Agric. Water Manag. 192, 33–44. https://doi.org/10.1016/j.agwat.2017.06.023.

Xu, X., Jiang, Y., Liu, M., Huang, Q., Huang, G., 2019. Modeling and assessing agro-hydrological processes and irrigation water saving in the middle Heihe River basin. Agric. Water Manag. 211, 152–164. https://doi.org/10.1016/j.agwat.2018.09.033.

Xue, J., Ren, L., 2017. Assessing water productivity in the Hetao Irrigation District in Inner Mongolia by an agro-hydrological model. Irrig. Sci. 35 (4), 357–382. https://doi.org/10.1007/s00271-017-0542-z.

Yang, G., Guo, P., Huo, L., Ren, C., 2015. Optimization of the irrigation water resources for Shijin irrigation district in north China. Agric. Water Manage. 158, 82–98. https://doi.org/10.1016/j.agwat.2015.04.006.

Yang, Y., Tian, F., 2009. Abrupt change of runoff and its major driving factors in Haihe River Catchment, China. J. Hydrol. 374 (3–4), 373–383. https://doi.org/10.1016/j.jhydrol.2009.06.040.

Yu, Y., Yu, R., Chen, X., Yu, G., Gan, M., Disse, M., 2017. Agricultural water allocation strategies along the oasis of Tarim River in Northwest China. Agric. Water Manage. 187, 24–36. https://doi.org/10.1016/j.agwat.2017.03.021.

Zdenek, Z., Petr, H., Karel, P., Daniela, S., Jan, B., Miroslav, T., 2017. Impacts of water availability and drought on maize yield - A comparison of 16 indicators. Agric. Water Manage. 188, 126–135. https://doi.org/10.1016/j.agwat.2017.04.007.

Zeng, X.T., Li, Y.P., Huang, G.H., Liu, J., 2017. Modeling of Water Resources Allocation and Water Quality Management for Supporting Regional Sustainability under Uncertainty in an Arid Region. Water Resour. Manage. 31 (12), 3699–3721. https://doi.org/10.1007/s11269-017-1696-4.

Zhang, B., 2009. Present water saving in agriculture in Xinzhou and strategies. Shanxi Water Resources 5, 36–37.

Zhang, Y., Arabi, M., Paustian, K., 2020. Analysis of parameter uncertainty in model simulations of irrigated and rainfed agroecosystems. Environ. Modell. Software 126, 104642. https://doi.org/10.1016/j.envsoft.2020.104642.

Zhao, J., Li, M., Guo, P., Zhang, C., Tan, Q., 2017. Agricultural Water Productivity Oriented Water Resources Allocation Based on the Coordination of Multiple Factors. Water 9 (7). https://doi.org/10.3390/w9070490.

Zuo, Q., Chen, Y., 2012. Method of typical year selection in multi-branches rivers with multi-stations. Journal of China Hydrology 32 (2), 1–4.